Applied Energy 299 (2021) 117104

Contents lists available at ScienceDirect

Applied Energy

journal homepage: www.elsevier.com/locate/apenergy

A multi-objective energy optimization in smart grid with high penetration of renewable energy sources

Kalim Ullah [a], Ghulam Hafeez [a,b,*], Imran Khan [a], Sadaqat Jan [c], Nadeem Javaid [d]

[a] Department of Electrical Engineering, University of Engineering and Technology, Mardan 23200, Pakistan
[b] Department of Electrical and Computer Engineering, COMSATS University Islamabad, Islamabad Campus 44000, Pakistan
[c] Department of Computer Software Engineering, University of Engineering and Technology, Mardan 23200, Pakistan
[d] Department of Computer Science, COMSATS University Islamabad, Islamabad 44000, Pakistan

ARTICLE INFO

Keywords:
Smart grid
Multi-objective energy optimization
Solar
Wind
Demand response programs
Incline block tariff

ABSTRACT

Energy optimization plays a vital role in energy management, economic savings, effective planning, reliable and secure power grid operation. However, energy optimization is challenging due to the uncertain and intermittent nature of renewable energy sources (RES) and consumer's behavior. A rigid energy optimization model with assertive intermittent, stochastic, and non-linear behavior capturing abilities is needed in this context. Thus, a novel energy optimization model is developed to optimize the smart microgrid's performance by reducing the operating cost, pollution emission and maximizing availability using RES. To predict the behavior of RES like solar and wind probability density function (PDF) and cumulative density function (CDF) are proposed. Contrarily, to resolve uncertainty and non-linearity of RES, a hybrid scheme of demand response programs (DRPS) and incline block tariff (IBT) with the participation of industrial, commercial, and residential consumers is introduced. For the developed model, an energy optimization strategy based on multi-objective wind-driven optimization (MOWDO) algorithm and multi-objective genetic algorithm (MOGA) is utilized to optimize the operation cost, pollution emission, and availability with/without the involvement in hybrid DRPS and IBT. Simulation results are considered in two different cases: operating cost and pollution emission, and operating cost and availability with/without participating in the hybrid scheme of DRPS and IBT. Simulation results illustrate that the proposed energy optimization model optimizes the performance of smart microgrid in aspects of operation cost, pollution emission, and availability compared to the existing models with/without involvement in hybrid scheme of DRPS and IBT. Thus, results validate that the proposed energy optimization model's performance is outstanding compared to the existing models.

1. Introduction

Recent studies regarding energy optimization intended that energy consumption can be reduced to 25%–35% without changing existing system infrastructure by optimizing power usage and power generation. One of the approaches for reducing power loss, pollution emission, and economically meeting users' needs is by renewable energy sources (RES) like wind and solar [1–3]. In recent years, a smart grid (SG) with high RES penetration has been introduced as a novel concept, and energy optimization has turned into an essential matter [4]. However, forecasting is indispensable prior to energy optimization [5]. One of the major challenging issues in energy optimization of RES, such as wind and solar, is uncertainty in their behavior means real-time generation is different from the forecasted one from these resources. Particularly due to the presence of uncertainty in energy generation from these RES, the SG operator's responsibility to maintain a balance between energy generation and consumption would confront some problems. The SG operators keep a certain amount of reserve as a backup to overcome uncertainty factors in energy generation and maintain security level at the required level [6].

The SG operators can overcome the problems described above by purchasing more energy from independent power producers or keeping fast-ramping fuel-based generators as a backup resource. However, these solutions are accompanied by some problems like increased operating cost and pollution emission [7]. Another solution is intended to resolve this problem and maintain a balance between energy generation and consumption by decreasing energy consumption during the shortage period caused by the prediction error of RES. One approach that SG operators adopt energy storage systems to manage energy shortages and maintain a balance between generation and consumption [8]. A strategy to overcome uncertainty in RES like wind and solar

* Corresponding author at: Department of Electrical and Computer Engineering, COMSATS University Islamabad, Islamabad Campus 44000, Pakistan.
E-mail addresses: ghulamhafeez393@gmail.com, ghulamhafeez@uetmardan.edu.pk (G. Hafeez).

https://doi.org/10.1016/j.apenergy.2021.117104
Received 28 January 2021; Received in revised form 12 April 2021; Accepted 20 May 2021
Available online 7 July 2021
0306-2619/© 2021 Elsevier Ltd. All rights reserved.

Nomenclature

A	Availability index
AMI	Advance metering infrastructure
BA	Bat algorithm
CDF	Cumulative density function
CO_2	Carbon dioxide
DSM	Demand side management
DST	Decision support tool
DGS	Distributed generation
DRPS	Demand response programs
DERS	Distributed energy resources
EV	Electric vehicles
EENS	Expected energy not served
FC	Fuel cell
FERC	Federal energy regulatory commission
Prs	Probability of scenarios
IBT	Incline block tariff
LMF	Linear mapping function
MOGA	Multi-objective genetic algorithm
MOWDO	Multi-objective wind driven optimization
MOPSO	Multi-objective particle swarm optimization
PCC	Point of common coupling
LC	Linear controllers
MINLP	Mixed integer non-linear programming
MILP	Mixed integer linear programming
NOx	Nitrogen oxide
OLM	Optimal load management
PDF	Probability density function
PSO	Particle swarm optimization
RES	Renewable energy sources
SOC	State of charge
SG	Smart grid
SO_2	Sulfur dioxide
VOLL	Value of lost load
WES	Wind energy system
MT	Micro turbine
$Rcon$	Residential consumers
$Ccon$	Commercial consumers
$Icon$	Industrial consumers
$(Rconmax, t)$	Residential max reduced load
$Rcon^max$	Maximum energy consumption of residential load
$Rcon_T$	Total energy consumption of residential load
$(Cconmax, t)$	Commercial max reduced load
$Ccon_T$	Total energy consumption of commercial load
$Ccon^max$	Maximum energy consumption of commercial load
$(Iconmax, t)$	Industrial max reduced load
$Icon_T$	Total energy consumption of industrial load
$Icon^max$	Maximum energy consumption of industrial load
$UOC(t)$	Uncertain operational cost
$COC(t)$	Certain operational cost
c_i	Solar irradiance
PR	Rated power
D	Early demand
δD	Demand not met
E_{ci}	Cut-in speed
E_r	Rated speed
E_{co}	Cut-off speed
E_{wind}	Actual wind speed
$PpE(ci)$	Output PV power
Ac	Solar arrays surface area
$w_i(T)$	Output power
$oi_i(T)$	Offered price
$S_i(T)$	DGS opening and closing period
$Reci^{DG}(T)$	Reserve cost of DGS
$RC_{j\,j,s}^{DR}(T)$	Running cost of DGS
$Recj^{DR}(T)$	Reserve cost of DRPS
$\mu(R_k)$	Number of solutions in current rank
N_k	Total number of solutions
R_k	Rank of solutions
μ_k	Number of solutions of the rank Rk
$\varsigma_{co,t}$	Amount of incentive payment to commercial consumer in each timeslot
$\varsigma_{in,t}$	Incentive payment to industrial consumer in each timeslot
R_k	Rank of solutions
dkj	Share fitness value
$\varsigma_{re,t}$	Incentive payment to residential consumer in each timeslot
δ and γ	PDF parameters
$\delta\gamma$	Measurement parameters
$\beta\gamma$	Shape parameters
η	PV efficiency
PVS	Photovoltaic system
co	Total number of commercial consumers

is demand response programs (DRPS), which is discussed in [9,10]. Federal energy regulatory commission (FERC) defined DRPS in two ways: (i) the program where consumers can change their energy usage pattern in response to the pricing signal offered by the SG operators, and (ii) the incentive payments intended to induce lower energy usage at times of high energy demand or when power system stability is endangered [11]. The former one is called price-based DRPS, and the latter one is known as incentive-based DRPS. For more in-depth understanding, see [12]. Recently, significant research studies have been conducted on implementing DRPS and modeling their role in handling the stochastic behavior of RES in energy optimization. DRPS are adopted in [13] to maintain a balance between energy generation and smart microgrid consumption with RES such as solar and wind. A particle swarm optimization (PSO) algorithm is employed to optimize the intended model's operating cost. However, pollution function is not considered while modeling the microgrid energy optimization problem. The DRPS is implemented in [14] to control the SG frequency integrated with RES. A wind–thermal energy scheduling in SG is evaluated using DRPS and stochastic programming to optimize operation cost, and pollution emission [15,16]. The DRPS is investigated in operation management of the SG integrated with wind turbine and photovoltaic cells in [17,18] using ε- constraint as a multi-objective optimization problem. The DRPS and spinning reserve are investigated in [19,20], respectively to cover the wind power shortage problem in the power system.

Alternatively, a mixed integer linear programming (MILP) method is employed in [21] to solve the energy optimization problem. However, the authors focused only on forecasting and ignored uncertainty accompanied by RES. An energy optimization strategy in SG integrated

with wind generation considering uncertainty is evaluated in [22]. The purpose of the authors is to maximize social welfare. However, the authors did not cater solar energy and incentive-based DRPS. A probabilistic model for energy optimization in SG with integrated wind and solar is evaluated in [23] to optimize operational cost and emission. They used beta probability density functions (PDF) and Rayleigh to model wind and solar behavior variation, respectively. A similar multi-objective energy management model integrated with RES is solved using a multi-objective particle swarm optimization (MOPSO) algorithm. The purpose of the authors is to optimize operational cost and pollution emission [24,25]. However, the intended model is suitable for the said scenario, and their performance is degraded with scalability. Similarly, in [26], a scenario tree method is utilized to solve the energy management problem. However, the modeling of solar irradiation is ignored in this study. Optimal energy management and modeling of a microgrid integrated with RES are evaluated in [27,28] by employing the mesh adaptive direct search method. However, in this study, uncertainty caused due to RES is not catered. A Monte Carlo technique based stochastic planning approach is intended in [29] for stochastic behavior modeling of wind energy. Furthermore, a DRPS considering wind energy influence as an operational storage in the electricity market is evaluated. In general, to overcome uncertainties accompanied by RES such as solar and wind energy, using reserve and ancillary services is as early as the emergence of these resources. Recently, significant research works on SG operation management have been conducted [30,31]. An expert energy optimization system is proposed in [32,33] for solar and wind connected with a microgrid to cover accompanied uncertainties and minimize operation cost and pollution emission. A smart energy optimization strategy based on a heuristic algorithm is proposed for grid-interactive microgrid [34] to optimize energy consumption and pollution emission and obtain net-zero energy buildings.

Since there are three primary objectives in smart microgrid energy optimization, like operating cost, pollution emission, and availability, the above references have investigated this research area from different perspectives and provide a good study for understanding the theme. Some studies catered uncertainties caused by RES from the forecasting error of wind and solar energy in a system using mathematical methods. On contrarily, some authors employed DRPS to tackle uncertainties accompanied by RES. Some studies catered to operating cost while others focused on pollution emission. However, considering only one aspect (operating cost or pollution emission or availability) is insufficient. Every aspect (operating cost, pollution emission, and availability) is of prime importance and can be catered simultaneously. Besides, all models are valuable assets of literature and capable of performing energy optimization. However, there is no universal mechanism that is effective in all aspects, and some mechanisms are better for some specific scenarios, conditions, and objectives. Furthermore, the existing literature methods can tackle uncertainties caused by RES like wind and solar and the non-linear behavior of demand-side participants. However, their performance is not satisfactory and estimated results are not up to the mark. Therefore, an optimal energy optimization mechanism is needed, capable of performing energy optimization by catering all aspects simultaneously and finding a solution to overcome uncertainties accompanied by the RES and behavior of demand-side participants.

With this study's motivation, a novel model is developed based on a multi-objective genetic algorithm (MOGA) and multi-objective wind-driven optimization (MOWDO) algorithm to solve energy optimization problems and cater operating cost, pollution emission, and availability simultaneously. The novelty and significant technical contributions of this work are outlined below:

- A novel hybrid scheme of DRPS and incline block tariff (IBT) is introduced to overcome uncertainty caused by solar and wind RES which are integrated with smart grid using the concept of parametrized cognitive adaptive optimization to obtain low cost, pollution emission and maximum availability of RES.
- An energy optimization model is developed utilizing MOGA and MOWDO with Pareto fronts criterion using the non-linear sorting fuzzy mechanism to solve the multi-objective energy optimization problem.
- PDF and CDF probabilistic models are employed through Monte-Carlo simulations to predict solar irradiation and wind speed to provide more explicit consent between planning and reality.
- Results utilizing the proposed model have proven optimal compared to the benchmark models in aspects of operating cost, pollution emission, and RES availability.

The remaining sections of the paper are organized as follows. The proposed energy optimization model is discussed in Section 2 and proposed and benchmark techniques are demonstrated in Section 3. The simulation results and discussions are reported in . Finally, the conclusion and future research directions are discussed in Section 4.

2. Proposed energy optimization model

A novel energy optimization model is proposed to minimize operating cost, pollution emission and maximize availability with and without involvement in hybrid scheme of DRPS and IBT using RES in the smart microgrid. The overall working implementation diagram of the proposed model is shown in Fig. 1. The proposed energy optimization model consists of subsystems, which are discussed in the following subsections.

2.1. Wind energy system

Energy demand is rapidly increasing to meet this rising energy demand without polluting the environment. Wind energy is beneficial energy, which is converted into electrical energy by employing wind turbines. Wind energy is based on the availability of wind, speed of the wind, wind turbine power curve, wind turbine shape, and turbine size. Wind energy is stochastic and intermittent containing high variation. Speed of wind is not the only variable that is affecting the power captured by the wind turbine uses for power generation. The correlation between speed of wind and direction of wind is equally important as the speed of wind captured by the wind turbine. Therefore, in this study, for wind speed prediction and correlation between speed of wind and direction of wind, PDF (Rayleigh) is used. In this work, it is predicted by Rayleigh distribution employing historical data [35], the PDF and cummulative distribution function (CDF) of Rayleigh distribution are as follows:

$$F_v(v_{wind}) = 1 - \exp\left[-\left(\frac{v_{wind}}{\delta^2\gamma}\right)^2\right] \tag{1}$$

$$f_v(v_{wind}) = \frac{2}{\delta^2\gamma} v_{wind} \times exp\left[-\left(\frac{v_{wind}}{\delta^2\gamma}\right)^2\right] \tag{2}$$

$$\begin{aligned} v_n &= \delta_\gamma \lambda(1+\tfrac{1}{2}) = \tfrac{1}{2}\delta_\gamma \lambda(\tfrac{1}{2}) = \tfrac{\sqrt{\pi}}{2}\delta_\gamma \\ \alpha_\gamma &= \tfrac{2}{\sqrt{\pi}}\delta_\gamma \end{aligned} \tag{3}$$

where v_n is the average wind speed of the particular area, the scale parameter is shown in Eq. (3). Therefore, in the case of returning $\beta\gamma$ to PDF and CDF, Rayleigh's model of WES will be achieved as a function of speed of wind according to Eqs. (4) and (5). The PDF and CDF curves are shown in Figs. 2 and 3.

$$F_E(E_{wind}) = \frac{\pi}{2}\frac{E_{wind}}{E^2{}_i}\exp(-\frac{\pi}{4})(\frac{E_{wind}}{E^2{}_i})^2 \tag{4}$$

$$F_E(E_{wind}) = 1 - \exp(-(\frac{\pi}{4})(\frac{E_{wind}}{E_i})^2) \tag{5}$$

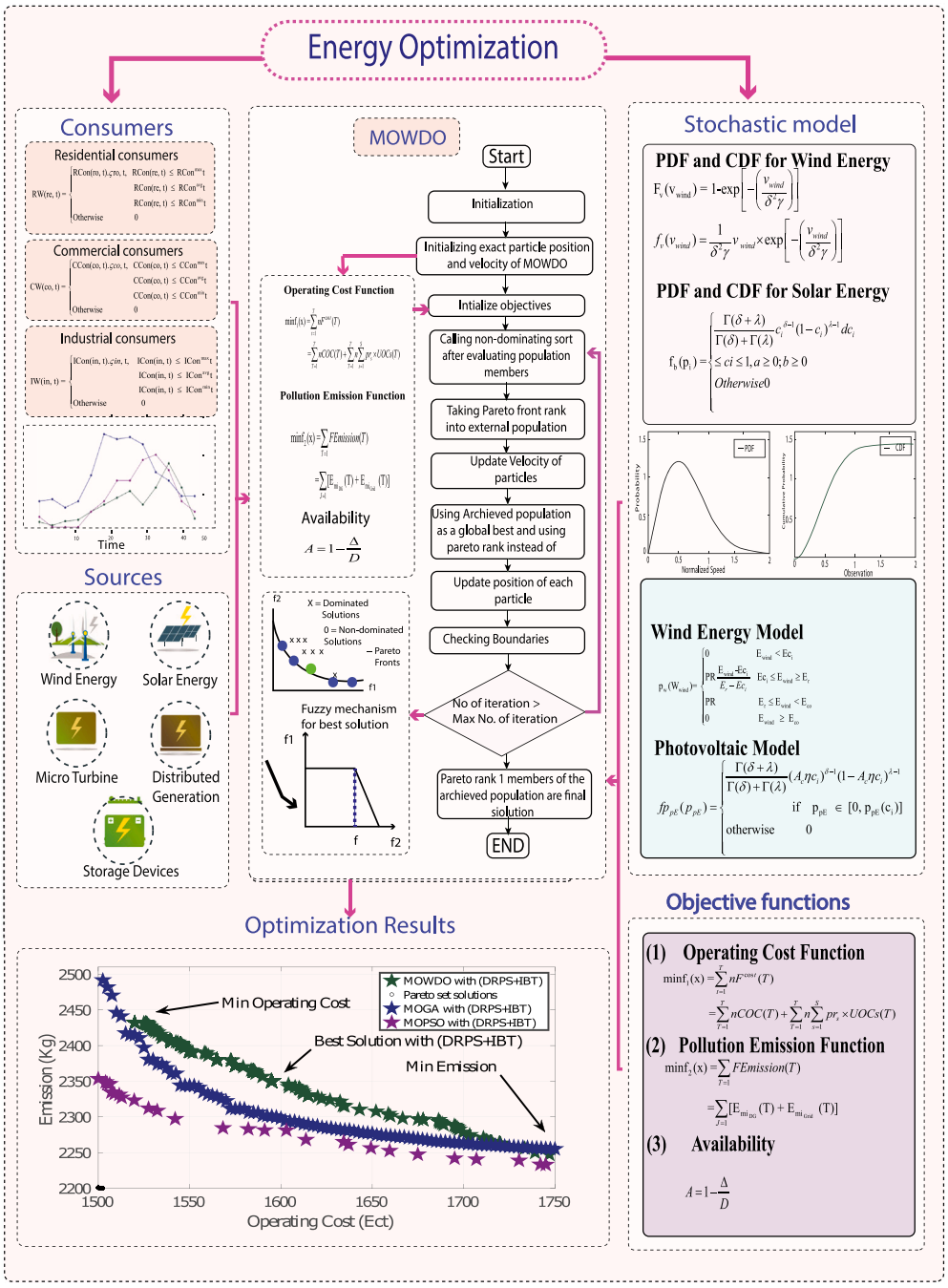

Fig. 1. Overall implementation of the proposed energy optimization model with high penetration of renewable energy sources engaging three service areas residential, commercial, and industrial in hybrid scheme of DRPS and IBT.

For certain WES, the output power is defined below [36]:

$$p_w(E_{wind}) = \begin{cases} 0 & E_{wind} < E_{ci} \\ PR\frac{E_{wind}-E_{ci}}{E_r-E_{ci}} & E_{ci} \le E_{wind} < E_r \\ PR & E_r \le E_{wind} < E_{co} \\ 0 & E_{wind} \ge E_{co} \end{cases} \quad (6)$$

where PR, E_{ci}, E_r, E_{co}, E_{wind} denotes rated power, cut-in speed, rated speed, cutoff speed and actual wind speed of wind turbine respectively. AIR403 type wind turbine is used in this study [37], where PR = 15 kW, E_ci = 3.8 m/s, E_co = 18 m/s, E_r = 17.5 m/s. Output power of WES can be obtained using Eqs. (4) and (6) through transformation theorem [38].

$$f\,p_w(p_w) = \begin{cases} 1-[F_E(v_\infty)-FE(E_{ci})], & p_w = 0 \\ (\frac{E_r-E_{ci}}{p_R}).(\frac{\pi}{2E^2{}_i}) \times (E_{ci}+(E_r-E_{ci}).\frac{p_w}{p_R}).. \\ \quad \times \exp\left[-\left(\frac{(E_{ci}+(E_r-E_{ci}).\frac{p_w}{p_R})^2}{\frac{2}{\sqrt{\pi}}E_m}\right)\right], \\ 0 < p_w < p_R \\ F_v(p_w)-F_v(v_r), & p_w = P_R \end{cases} \quad (7)$$

2.2. Photovoltaic system

The PVS system converts sunlight into electrical energy. Probabilistic models PDF and CDF are used to models the behavior of solar irradiance as illustrated in Eq. (8) and (9) taken from [39,40].

$$fb(p_i) = \begin{cases} \frac{\Gamma(\delta+\lambda)}{\Gamma(\delta)\Gamma(\lambda)} c_i^{\delta-1}(1-c_i)^{\lambda-1} dc_i \\ \qquad 0 \le c_i \le 1, a \ge 0; b \ge 0 \\ 0 \qquad otherwise \end{cases} \tag{8}$$

$$F_d(c_i) = \int_0^{ci} \frac{\Gamma(\delta+\lambda)}{\Gamma(\delta)\Gamma(\lambda)} c_i^{\delta-1}(1-c_i)^{\lambda-1} dc_i \tag{9}$$

where c_i shows solar energy in kw/m^2. δ and λ are PDF parameters that may find the mean value of the standard deviation of solar energy data and are utilized as follows:

$$\delta = \eta\left(\frac{\sigma(1+\sigma)}{\delta^2} - 1\right) \tag{10}$$

$$\lambda = (1-\sigma)\left(\frac{\sigma(1+\sigma)}{\delta^2} - 1\right) \tag{11}$$

Eq. (12) shows the amount of solar irradiance is converted into solar energy in two days [41].

$$p_{pE}(c_i) = A_c.\eta.c_i \tag{12}$$

where $P_pE(c_i)$ shows the output power comes from solar energy system in (kW), irradiance c_i, Ac is the surface area of solar arrays in m^2 and η is solar energy system efficiency. Eq. (8) indicates, PDF fp_pE is output power of solar energy system as follows:

$$fp_{pE}(p_{pE}) = \begin{cases} \frac{\Gamma(\delta+\lambda)}{\Gamma(\delta)\Gamma(\lambda)} (A_c\eta c_i)^{\delta-1}(1-A_c\eta c_i)^{\lambda-1} \\ \qquad if\, p_{pE} \in [0, p_{pE}(c_i)] \\ 0 \qquad otherwise \end{cases} \tag{13}$$

2.3. Hybrid wind–solar power system

The hybrid power system is a combination of WES and PVS. The power generated by the hybrid power system is equal to the sum of power generated from solar and wind energy system, which is mathematically modeled as follows:

$$P_H = p_{wind} + p_{solar} \tag{14}$$

where *Pwind* and *Psolar* are independent variables according to Eqs. (6) and (12). P_H is hybrid power generated, which is modeled as convolution between PDF of p_{wind} and p_{solar} as follows [42].

$$f_h(P_H) = fp_{wind}(Pp_{wind}) * fp_{solar}(Pp_{solar}) \tag{15}$$

It is non-trivial to use the continuous PDF mathematics. Therefore, the Monte-Carlo simulation is employed here to get distinct conditions; however, creating different contexts also adds to the mathematical problem's complexity. The proper strategy to prevent math difficulty is to extract a continuous PDF and execute it in different parts. In the proposed model, we divided PDF into eight parts per time slot to provide the desired power.

2.4. Proposed hybrid scheme of demand response programs and incline block tariff

Electric utility companies initiate DRPS to encourage consumers to participate in energy optimization to reduce cost. Electric utility companies either give flexibility to consumers to shift their load from on-peak hours to off-peak hours or directly control their load through DRPS by providing incentives. The DRPS has high flexibility, and all consumers (residential, commercial, and industrial) concentrate all their activities to relatively low price hours. Thus, there is a possibility of building peaks during off-peak hours (rebound peaks), which overloads the entire power system that leads to instability or even blackout. In this regard, this work introduced a hybrid scheme by combining DRPS and IBT, where incentive payment could be different within the same hour based on the total energy consumption, which effectively reduced rebound peaks and enhanced the stability of the entire power system. Besides, the demand-side consumers like industrial, residential, and commercial are involved in our proposed hybrid scheme to overcome uncertainty and rebound peaks problems. The hybrid scheme of DRPS and IBT set two incentive payment levels, and energy consumption and their corresponding cost changes every hour. The hybrid scheme for residential, commercial, and industrial consumers is mathematically modeled in Eqs. (16), (17), and (18), respectively.

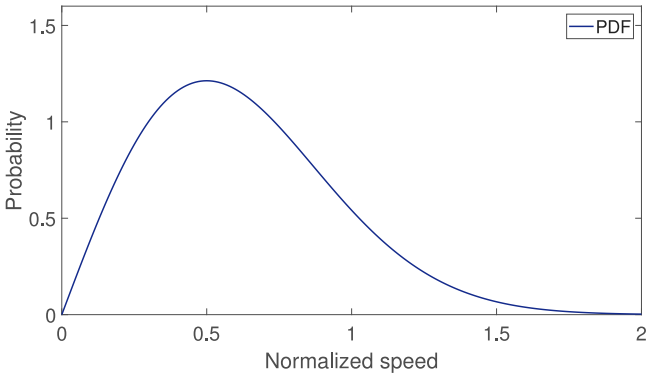

Fig. 2. PDF:Wind speed distribution model.

$$\mathrm{RW(re,t)} = \begin{cases} \mathrm{RCon(re,t).}\varsigma re_1 & \text{if } 0 \le \mathrm{RCon}_T \le \mathrm{RCon}^{\max} \\ \mathrm{RCon(re,t).}\varsigma re_2 & \text{if } \mathrm{RCon}_T > \mathrm{RCon}^{\max} \\ 0 & \text{otherwise} \end{cases} \tag{16}$$

$$\mathrm{CW(co,t)} = \begin{cases} \mathrm{CCon(co,t).}\varsigma co_1 & \text{if } 0 \le \mathrm{CCon}_T \le \mathrm{CCon}^{\max} \\ \mathrm{CCon(co,t).}\varsigma co_2 & \text{if } \mathrm{CCon}_T > \mathrm{CCon}^{\max} \\ 0 & \text{otherwise} \end{cases} \tag{17}$$

$$\mathrm{IW(in,t)} = \begin{cases} \mathrm{ICon(in,t).}\varsigma in_1 & \text{if } 0 \le \mathrm{ICon}_T \le \mathrm{ICon}^{\max} \\ \mathrm{ICon(in,t).}\varsigma in_2 & \text{if } \mathrm{ICon}_T > \mathrm{ICon}^{\max} \\ 0 & \text{otherwise} \end{cases} \tag{18}$$

where *re*, *co* and *in* are residential, commercial and industrial consumers; RCon_T, CCon_T, and ICon_T denote total energy consumption of residential, commercial, and industrial consumers, respectively; *RCon (re, t)*, *CCon (co, t)* and *ICon (in, t)* shows reduced loads which are planned for each consumer in time slot t; $RCon^{\max}$, $CCon^{\max}$ and $ICon^{\max}$ are maximum energy consumption, represents threshold power consumption of IBT, respectively. ς_{re_1}, ς_{co_1}, and ς_{in_1} indicate overall incentive payment level that should be greater than ς_{re_2}, ς_{co_2}, and ς_{in_2} incentive payment level of residential, commercial, and industrial consumers, and *RW (re, t)*, *CW (co, t)*, and *IW (in, t)* shows costs due to the reduction of the load by each consumers during the proposed load reduction. The applications of hybrid scheme DRPS and IBT implementation involves to decrease electricity cost, avoid rebound peaks formation, avoid risk management, avoid uncertainty, and provide flexibility in energy optimization.

2.5. Objective functions

In this study, the proposed energy optimization model will cater three objectives: operational cost, pollution emission, and availability

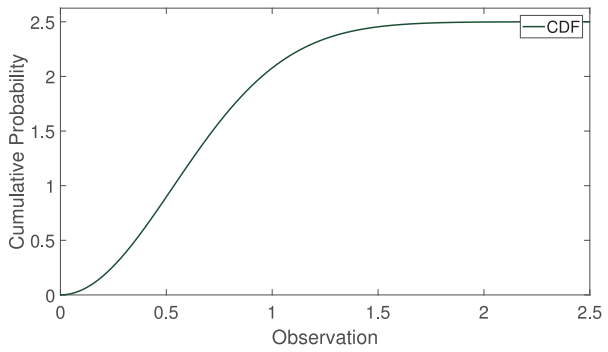

Fig. 3. CDF:Wind speed distribution model.

Table 1
Price and quantity offered packages for hybrid scheme of DRPS and IBT.

	Quantities in kW Price in Ect/kWh	Quantities in kW Price in Ect/kWh	Quantities in kW Price in Ect/kWh	
DRPS+IBT 1	0–10 0.19	10–20 0.23	20–50 0.29	50-70 0.40
DRPS+IBT 2	0–10 0.03	10–20 0.07	20–30 0.30	30-60 0.45

simultaneously in two cases. In case I, the proposed model's main objectives are to minimize the operation cost and pollution emission with and without involvement in the hybrid scheme of DRPS and IBT scheme. Similarly, in case II, operating cost and availability with and without involvement in the hybrid scheme of DRPS and IBT scheme is catered. The proposed model uses MOWDO and MOGA to optimize case I and case II's desired objectives. The detailed discussion is as follows:

2.5.1. Operating cost function

The operating cost is divided into two categories: Certain operating cost and uncertain operating cost. The uncertain operating cost includes start-up and running costs of distributed generations (DGS). The certain operating cost includes reserve cost provided by DGS, DRPS, and power cost, which is purchased/sold, from/to the utility and the probability of scenarios Pr_s are affected by uncertainty in the wind and solar parameters in each case. The uncertain operating cost includes running costs for the DGS unit, reducing the load due to the DRPS+IBT implementation, the costs related to the value of lost load (VOLL) and the expected energy not served (EENS) cost for consumers.

$$\begin{aligned} \min f_1(x) &= \sum_{T=1}^{T} nF^{\cos t}(T) = \sum_{T=1}^{T} nCOC(T) \\ &+ \sum_{T=1}^{T} n \sum_{s=1}^{S} p_{r_s} \times UOC_s(T) \end{aligned} \tag{19}$$

where Pr_s is the probability of scenarios. Certain and uncertain operating cost functions are defined in Eqs. Eq. (20) and (21), respectively.

$$\begin{aligned} &COC(T) \sum_{i=1}^{N_{DG}} [w_i(T) o_i(T) s_i(T) + QU_i(T) \\ &.|s_i(T) - s_i(T-1)| + {ReC_i}^{DG}(T)] \\ &+ \sum_{j=1}^{J} {ReC_j}^{DR}(T).s_{buy}(T).W_{Grid-buy}(T) \\ &.oi_{Grid-buy}(T) - I_{Sell}(T) W_{Grid-buy}(T) \end{aligned} \tag{20}$$

$$\begin{aligned} UOC(T) = \sum_{i=1}^{N_{DG}} [{RCi^{DG}}_{i,s}(T) + \sum_{j=1}^{J} {RCj^{DR}}_{j,s}(T) \\ + EEN_s(T) \times VOLL(T) \end{aligned} \tag{21}$$

where $w_i(T)$ and $oi_i(T)$ are output power and the given price for the i_{th} units in T_{th} time, $s_i(T)$ represents i_{th} DGS opening and closing state during the T_{th} period, $QU_i(T)$ indicates the operation and closing cost for the i_{th} unit during the T_{th} time, ${Rec_i}^{DG}(T)$, ${Rec_j}^{DR}(T)$ are reserved cost of i_{th} DGS, DRPS+IBT for the j_{th} load during the T_{th} time, $W_{Grid-buy}(T)$ and $W_{Grid-Sell}(T)$ represents exchange power with utility during time T_{th} time, $w_{Grid-buy}(T)$ and $w_{Grid-sell}(T)$ indicates the offered-price for exchange power with utility in electric markets in T_{th} time period. ${RCi_{i,s}}^{DG}(T)$ and ${RC_{j_{j,s}}}^{DR}(T)$ shows running costs of i_{th} DGS units and the costs because of reduced loads by j_{th} DRPS during T_{th} time in s_{th} scenarios, *EMNS(T)* and *VOLL(T)* are expectation energies not serve in s_{th} scenarios in T_{th} time and value of lost load in T_{th} time period, respectively. According to Eq. (17), S is a state variable which contains the actual power generated by DGS, charging and discharging of battery power and the variable active power through the mounting grid. In terms of operating costs in the proposed model, it is assumed that DGS, as well as DRPS+IBT, are the spinning reserve suppliers by suppressing uncertainties caused by wind and solar RE. Therefore, the reserved cost is taken as a probability in every start component of the objective functions.

2.5.2. Pollution emission function

The emission function involves activities such as the amount of emission produced by DGS and the quantity of emission caused by the grid during purchase. Pollutants include carbon dioxide, sulfur dioxide, and nitrogen dioxide are represented by CO_2, SO_2, and NO_2, respectively, as well as a statistical model for the pollution function, can be defined as follows.

$$\begin{aligned} \min f_2(x) &= \sum_{T=1} F^{Emission}(T) \\ &= \sum_{J=1} [{E_{mi}}_{DG}(T) + {E_{mi}}_{Grid}(T)] \end{aligned} \tag{22}$$

DGS pollution is calculated as follows:

$$\begin{aligned} Emi^{DG}(T) = \sum_{j=1}^{N_{DG}} {E_{CO2}}^{DG}(j) + {E_{SO2}}^{DG}(j) + {E_{NOx}}^{DG}(T) \\ \times {P_j}^{DG}(T) \end{aligned} \tag{23}$$

where ${E_{CO2}}^{DG}(j)$, ${E_{SO2}}^{DG}(j)$ and ${E_{NOx}}^{DG}(T)$ shows emissions generated due to CO_2, SO_2, and NO_2, by j_{th} DGS respectively; is measured in *K.g/Mwh*. Similarly, the pollution caused by the grid during power purchase can be written as follows:

$$\begin{aligned} Emi_{Grid}(T) = ({E_{CO2}}^{Grid} + {E_{SO2}}^{Grid} + {E_{NOx}}^{Grid}) \\ \times P_{Grid}(T) \end{aligned} \tag{24}$$

2.5.3. Availability function

Availability of the system deals with the capacity of the system to deliver power to consumers. The availability of the system in a specific duration is presented by [43], which is given as follows.

$$A = 1 - \frac{\Delta}{D} \tag{25}$$

where A, D, ΔD represents the availability index, early demand and demand not met, respectively. ΔD can be defined as follows.

$$\Delta D = \sum_{t=1}^{T} \begin{pmatrix} {P_{batt}}_{Min}(t) - {P_{batt}}_{SOC}(t) \\ -\begin{pmatrix} P_{solar}(t) + P_{wind}(t) \\ +P_{net}(t) - P_D(t) \end{pmatrix} \times U(t) \end{pmatrix} \tag{26}$$

where ΔD shows the demand not met, $P_{batt}(t)$, $P_{SOC}(t)$ represents minimum charge of proposed battery, status of charge of a battery in time slot t, $P_D(t)$, $U(t)$ indicates the total demand in time t and step function, respectively. From Eq. (26), if the supplied power is greater than or equal to demand, the above function will be equal to zero. However, if the power provided and power demanded are met, the function is equal to 1.

2.6. Problem constraints

The operation of the smart microgrid is ensured using following constraints.

2.6.1. Power-network constraints

The total energy produced by DGS and the power grid is equal to the overall demand load.

$$\sum_{l=1}^{N_{DG}} P_{DG,\,i,s}(T) + P_{Grid,s}(T) = \sum_{i=1}^{N_s} P_{Demand\,l,s}(T) - P_{DR,s}(T) \tag{27}$$

$P_{Demand_{l,s}}$ is L_{th} demands level in T_{th} time and s_{th} scenarios. In Eq. (28), $P_{DR}(t)$ is an actual power involvement in DRPS+IBT and given as:

$$P_{DR,x}(T) = \sum_{re} RCon(re,t,\mathrm{x}) + \sum_{co} CCon(co,t,\mathrm{x}) + \sum_{in} ICon(in,t,\mathrm{x}) \tag{28}$$

2.6.2. Reserves and DGS power constraints

Energy produced by DGS:

$$P^{min}{}_{DG,x}.I(x,t) \le P_{DG}(x,t,s) \le P^{max}{}_{DG,x}.I(x,t) \quad \forall x,t,s \tag{29}$$

$$R_{DG}(x,t) \ge P_{DG}(x,t,s) - P_{DG}(x,t,0) \quad \forall x,t,s \tag{30}$$

2.6.3. Battery ON-OFF constraints

Battery used in proposed model are:

$$\begin{aligned} W_s(T) &= W_s(T-1)1 \\ &\quad + x_{charge}(T) q_{charge}(T) \Delta T.I_{charge} \\ &\quad - \frac{1}{x_{discharge}} q_{discharge}(T) \Delta T.I_{discharge} I_{discharge}(T) + \\ &\quad I_{charge}(T) \\ &\le 1 W_{s,minimum} \le W_s(T) \le W_{s,maximum} q_{charge}(T) \\ &\le q_{charge,maximum}; q_{discharge}(T) \le q_{discharge,maximum} \end{aligned} \tag{31}$$

where, $W_s(T)$ and $W_s(T\text{-}1)$ indicates power stored in battery at time T and $(T\text{-}1)$ respectively, q_{charge} and $q_{discharge}$ are the battery charge and discharge cycle during time ΔT respectively, x_{charge} and $x_{discharge}$ is charge and discharge allowed by battery during the whole cycle, $(W_s, minimum)$ and $(W_s, maximum)$ indicates lower and higher power store by battery and $(q_{chrge}, maximum)$, $(q_{discharge}, maximum)$ are maximum charge and discharge of battery during ΔT period [44].

In this model, battery storage system involvement aims to provide back-up power to the smart microgrid. If the source power goes down, the battery offers services to the smart microgrid and storing energy in off-peak hours. The battery storage system's applications balance the grid power, save the smart microgrid's cost, and assist the smart microgrid when other sources of power go down. In this way, smart microgrid efficiency increases.

2.7. Typical smart microgrid

The smart microgrid system is shown in Fig. 4 consisting of industrial, commercial, and residential consumers, with the participation of DGS, FC, MT, WES, PVS, battery, and utility. The smart microgrid can be operated in stand-alone mode or conjunction with the main power grid [45,46]. The development of smart microgrid is a part of SG concept, therefore, both have some common objectives in energy optimization such as DRPS and green technology implementation, reliable and secure energy provision [46]. The parametrized cognitive adaptive optimization and control approach is used to integrate predicted RESs with the smart microgrid that provides balance power to demand-side consumers. The inclusion of this technique in the model is due to its consistent, fastness and "plug-n-play" behavior, and it is suitable for any complex system, whether it is small or large. The parametrized cognitive adaptive optimization is applied to the set of controllers shown in Fig. 4. The signals are collected at point of common coupling (PCC) and deliver to parametrized cognitive adaptive optimization based central controllers. The center controllers control signals in real-time according to the situation and operation inside the smart microgrid, as shown in Fig. 4. There are different linear controllers (LC) which take control signals from central controller to reduce the complexity of system design and optimize the performance of the smart microgrid. The installation characteristics are listed in Table 2, where DGS offered price in (Ect/kWh), start/shutting-down cost in (Ect), minimum power P_{min} in (kW), maximum power P_{max} in (kW), CO_2 in (kg/MWh), SO_2 in (kg/MWh) and NO_x in (kg/MWh) pollution produced by DGs and utilities, low and high energy generation [47].

3. Existing and proposed multi-objective optimization methods

In this work, two multi-objective algorithms like MOGA and MOWDO with Pareto fronts criterion using the non-linear sorting fuzzy mechanism compared to existing multi-objective particle swarm optimization (MOPSO) algorithm are employed for energy optimization. The detailed description of the adapted and existing algorithms are as follows.

3.1. Multi-objective particle swarm optimization algorithm

The multi-objective energy optimization problems include conflicting objectives under equality and inequality constraints, which must be solved simultaneously. In this work, three conflicting objectives like operating cost, pollution emission, and availability must be optimized simultaneously.

$$minf(Y) = [F_1(Y), F_2(Y).....F_N(Y)]^T \tag{32}$$

subject to:

$$\begin{cases} k_i(Y) < 0 \quad i = 1,2,3....., N_{ueq} \\ vi(Y) = 0 \quad i = 1,2,3...., N_{eq} \end{cases} \tag{33}$$

where $f(Y)$ contains an objectives function and Y consist of variables of an optimization, $F_i(Y)$ is objectives function, $k_i(Y)$ and $v_i(Y)$ are equalities and inequalities constraint and number of objective functions is denoted by N. For a multi-objective optimization problem, either x or y will be one of two possible solutions. One will supersede the other. Therefore, when the following two functions are matched, Y will dominated Z.

$$\begin{aligned} &\forall m \in \{1,2,3.....,n\}, \quad f_m(Y) \le f_m(Z) \\ &\exists n \in \{1,2,3.....,n\}, \quad f_n(Y) < f_n(Z) \end{aligned} \tag{34}$$

Hence, Pareto-fronts solution can be found with a non-dominated solution (desired). Here, the Pareto-front optimization concept is executed on particle swarm optimization algorithm [48]. Optimization of operating cost and pollution emission, and operating cost and availability using RES with/without DRPS+IBT through MOPSO [49]. steps of MOPSO:

Step 1: Initialize and define inputs to algorithm.
Step 2: Calculate sources power from equations.
Step 3: Create populations from set $XT=[X1, X2, \ldots, XT]$.
Step 4: Applying power dispatched technique for creating populations and calculations of fitness function.
Step 5: Identifying non-dominated solutions.
Step 6: Separates non-dominate solution and store it in archives.
Step 7: Selecting leader from non-dominated sort. Criterion to select leader from non-dominate sort is: Divide the require spaces in equal pieces and apply PDF to every single space. Therefore, roulette wheel will select the leader onward.
Step 8: Update particles velocities and positions in right direction.

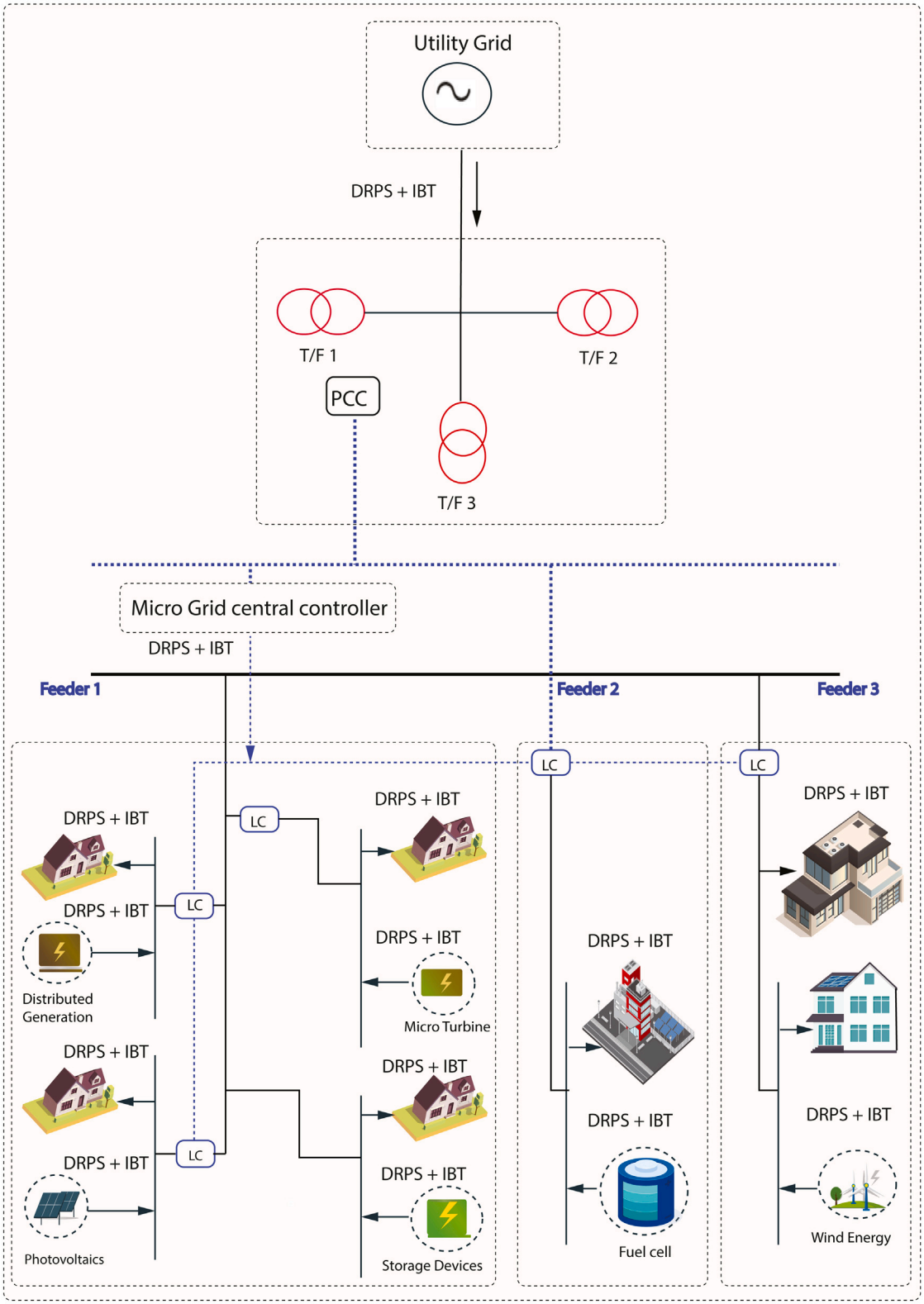

Fig. 4. Real-life practical schematic diagram of smart microgrid.

Step 9: Regenerating an every particles optimal position. Positions are compared with previous positions.

$$p_{best,j}(t+1) = \begin{cases} p_{best,j}(t) & p_{best,j}(t) < X_j(t+1) \\ X_j(t+1) & X_j(t+1) < p_{best,j}(t) \\ select\ randomly & \\ (p_{best,j}(t)\ or\ X_j(t+1))\ otherwise & \end{cases} \quad (35)$$

Step 10: Non-dominated solutions are added.

Step 11: Dominated solution.

Step 12: Removing exceeded members if exceeded then given numbers.

Step 13: Best possible solutions.

For choosing the best possible solution, Pareto fronts criterion using non-linear sorting fuzzy mechanism is used that finds a suitable location of variables in the archive. σ_i^k indicates an optimal number of objective

Table 2
Offer prices and pollution emission coefficients of distributed generation sources.

Units	Types	Offer price (Ect/kWh)	Start/Shutting-down Cost(Ect)	CO2 (kg/MWh)	SO2 (kg/MWh)	NOx (kg/MWh)	P_{min} (kW)	P_{max} (kW)
1	Diesel	0.586	0.15	890	0.0045	0.23	30	300
2	MT	0.457	0.96	720	0.0036	0.1	6	30
3	FC	0.294	1.65	440	0.003	0.0075	3	30
4	PVS	2.584	0	0	0	0	0	25
5	WES	1.073	0	0	0	0	0	15
6	Battery	0.38	0	10	0.0002	0.001	−30	30
7	Utility	–	0	950	0.5	2.1	−30	30

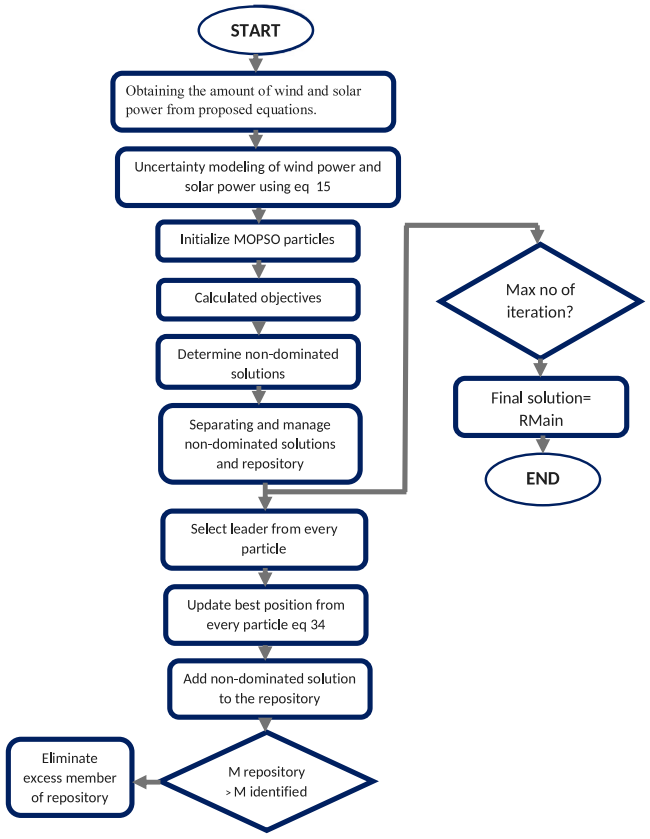

Fig. 5. Multi-objective particle swarm optimization algorithm implementation flow chart.

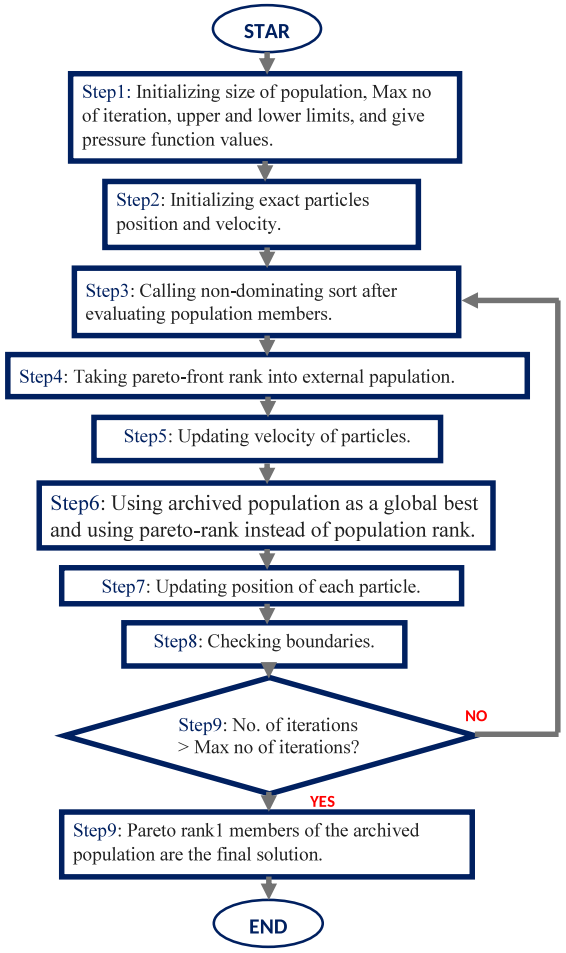

Fig. 6. Multi-objective wind-driven optimization algorithm implementation flow chart.

functions j, Pareto-fronts k and is given as:

$$\sigma_j^{\,k} = \begin{cases} 1 & f_j \le {f_j}^{\min} \\ \frac{{f_j}^{\max} - f_j}{{f_j}^{\max} - {f_j}^{\min}} & {f_j}^{\max} < f_j < {f_j}^{\min} \\ 0 & f_j \ge {f_j}^{\max} \end{cases} \tag{36}$$

The upper and lower bounds of objective function j are ${f_j}^{\max}$ and ${f_j}^{\min}$. These values are calculated using optimization results for each objective function. σ_i^k ranges in [0, 1] where $\sigma_i^k = 0$ represent incomplete solutions in given functions, where $\sigma_i^k = 1$ represent complete solutions. MOPSO flow chart is shown in Fig. 5.

3.2. Multi-objective wind-driven optimization algorithm

The multi-objective energy optimization problems include conflicting objectives under equality and inequality constraints, which must be solved simultaneously. In this work, three conflicting objectives like operating cost, pollution emission, and availability must be optimized simultaneously. MOWDO algorithm is based on position and velocity consisting of 5 main functions: Schaffer function, Kita function, Kursawe function, ZDT1 and ZDT4 functions. The proposed multi-objective algorithm aims to optimize operating cost, pollution emission, and availability. Moreover, the operating cost is a non-convex optimization problem. Therefore, to avoid local minima, we increase the probability of exploration (global minimization) more than the probability of exploitation (local minimization) in the search space. The particle converges to global minimization, and local minimization is avoided for operating cost optimization. The MOWDO algorithm flow chart is shown in Fig. 6.

MOWDO algorithm uses Pareto set ranks to find the best possible solution with and without involvement in hybrid scheme DRPS and IBT [50].

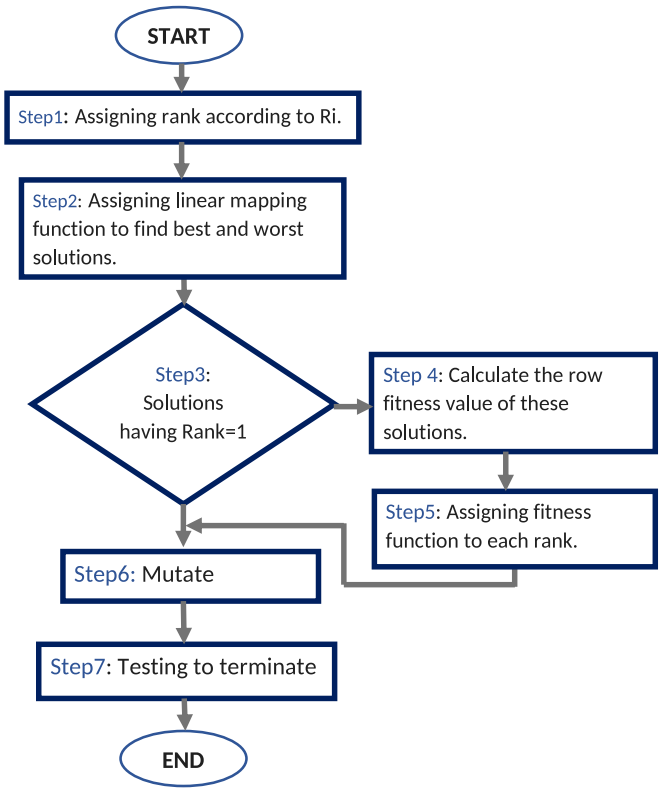

Fig. 7. Multi-objective genetic algorithm implementation flow chart.

3.2.1. Schaffer function

In this function, limits of variables are $[-10^3, 10^3]$, and optimized solution ranges [0,2]. Schaffer functions are:

$$f_1(k) = k^2, \quad f_2(k) = (k-2)^2 \tag{37}$$

3.2.2. Kita function

Here, the limits of variables are [0, 7]. Kita multi-objective functions are:

$$f_1(k_1, k_2) = -{k_1}^2 + k2 \tag{38}$$

and

$$f_2(k_1, k_2) = \frac{k_1}{2} + k2 + 1 \tag{39}$$

subject to:

$$\frac{k_1}{6} + k_2 \le \frac{13}{2}, \frac{k_1}{2} + \frac{15}{2}, 5k_1 + k_2 \le 30 \tag{40}$$

This function is used to utilize pressure effect.

3.2.3. Kursawe function

Here, the limits of variables are [−5, 5]. Kursawe multi-objective functions are:

$$f_1(k) = \sum_{j=1}^{N-1} (-10\exp(-0.2\sqrt{{k^2}_i + {k^2}_{j+1}})) \tag{41}$$

$$f_2(k) = \sum_{j=1}^{N} |{k_j}|^{0.8} + 5\sin({k^3}_j) \tag{42}$$

3.2.4. ZDT1 function

Here, variable limits are [0, 1]. ZDT1 multi-objective functions are:

$$f_1(k) = k_1$$
$$and$$
$$f_2(k) = g(k[1 - \sqrt{\tfrac{k_1}{g(k)}}]) \tag{43}$$
$$where \quad g(k) = 1 + 9(\frac{\sum_{j=2}^{N} k_i}{(N-1)})$$

3.2.5. ZDT4 function

Here, variable limits are $k1 = [0, 1]$, and $kj = [-5, 5]$ for j=2,3…,n. ZDT4 multi-objective functions are:

$$f_1(k) = k_1$$
$$and$$
$$f_2(x) = g(k)\left[1 - \sqrt{\left(\tfrac{k_1}{g(k)}\right)}\right] \tag{44}$$
$$and,$$
$$g(k) = 1 + 10(N-1) + \sum_{i=2}^{N} ({k^2}_j - 10\cos(4\pi k_j))$$

Following are the steps for proposed MOWDO algorithm.

Step 1: Initializing population size (number of population), iterations (maximum number of iteration for an optimized results), limits (maximum and minimum bounds) and defining pressure function (initialize pressure function given to MOWDO according to the proposed conditions) to the algorithm.

Step 2: Initializing particle's position (the current particles position which will be used ahead in the process in such a way that it will be compared with the new position of the particles) and particle velocity (v_{old}) (similarly the current velocity (v_{old}) of particles which will be used ahead in the process in such a way that it will be compared with the new velocity (v_{new}) of the particles) to MOWDO.

Step 3: Evaluating population members and calling non-dominated sort.

Step 4: Taking pareto-front members into external population.

Step 5: Updating velocity (in this step the particles velocity are updated, meaning the particles have new velocity (v_{new}).

Step 6: Using archived population as global best.

Step 7: Taking pareto-front instead of population rank.

Step 8: Updating position.

Step 9: Checking boundaries (limits).

Step 10: Checking maximum iteration of the MOWDO.

Step 11: If reached to maximum iteration, then Pareto-rank members of the archive population are the final solution. If not reached to maximum iteration then algorithm back to step 3 as shown in the flow chart in Fig. 6.

3.3. Proposed method: Multi-objective genetic algorithm

MOGA algorithm flow chart is shown in Fig. 7. MOGA use the non-dominated classification of the GA population and at the same time maintain diversity in non-dominated solutions [51].

The solutions which are near to Pareto optimal front are ranked equal to 1 are proposed. These solutions are optimal solutions. Similarly, all other solutions are ranked accordingly, based on their location. To find the rank of a solution, the following equation is used:

$$R_k = 1 + N_K \tag{45}$$

where R_k indicates the rank of solutions and N_K represents that how many solutions are there which can dominate the solution k, if a large number of solutions dominates, it means that the rank is higher. To combine more than one objective, the equation as follows:

$$F(X) = m_1 \cdot F_1(X) + \cdots . + m_j \cdot F_j(X) + \cdots \ldots + m_N f_N(X) \tag{46}$$

Algorithm 1: Pseudo-code of the multi-objective wind-driven optimization algorithm for energy optimization

Desired results:
Optimized operating cost and pollution emission, operating cost and availability ;
Initialization:
Population size, maximum iteration, boundaries, pressure function, particles positions;
Max velocity for MOWDO (v_{old}) = ±[0.5];
Implementation:
Evaluate pressure function for each member in population during each iteration;
Assign Pareto-front sets to every member of the population based on sorting using equation;
This Pareto-fronts information is in equation;

$$U_v = (1-k)U_b - gX_b + \left|\frac{j-1}{j}\right| RT(X_{max} - X_b) \times \frac{1}{j} k \times u_k{}^{otherd}$$

Rank 1 are the archived population members with Pareto-fronts;
Equation

$$U_v = (1-k)U_b - gX_b + \left|\frac{j-1}{j}\right| RT(X_{max} - X_b) \times \frac{1}{j} k \times u_k{}^{otherd}$$

Shows global best solutions so far with the non-dominated Pareto-fronts;
Update velocity;
Check boundaries with termination;
while *iteration < Max iteration* **do**
  for *j=1* **do**
    Check Pareto fronts information;
    if *Iteration=250?* **then**
      Pareto rank1 members of the archived population are the final solution;
      otherwise, back to step no 3 shown in MOWDO flow chart in Fig. 6
    end
    if *Iteration not equal to 250?* **then**
      Go to step 1 shown in Fig. 6;
    end
    if *fitness values > desired values* **then**
      Go to step 1 shown in Fig. 6;
    end
  end
  for *k = 1* **do**
    for *j = 1* **do**
      Calculate fitness coefficients;
      Check Pareto fronts;
      Calculate final best results;
    end
  end
end

where X is string of the rank, $F(X)$ is fitness function, $F_j(X)$ is j_{th} objective function and m_1 is a constant weight which indicates objectives function. The operating cost is non-convex optimization problem, therefore, to avoid local minima, in the search space, we increase the probability of exploration (global minimization) more than the probability of exploitation (local minimization). The particle converges to global minimization and local minimization avoided for operating cost optimization. Flow chart of proposed method MOGA is shown in Fig. 7 and stepwise procedure of MOGA is as follows.
Step 1: Assigning rank according to *Rk*.
Step 2: Using linear mapping function (LMF) to assign row fitness to each solution. Linear mapping function will assign the row fitness, also assign the row fitness function for the worst solutions.
Step 3: Calculating the average of row fitness values for each rank solutions. If the rank is 1 then checked the number of solutions having rank 1, take the average of row fitness value of these solutions.
Step 4: Applying crossover to each of assign values to produce new string.
Step 5: Applying mutate.
Step 6: Algorithm returns to step number 1, if satisfying conditions are not valid.

Now here we discussed that how to assign fitness values to MOGA.
MOGA fitness assignment: Assign fitness values are calculated as follows:
Step 1: Choose σ_{share}, which is a constant variable, denotes that how much distance is considered between two solutions. If σ_{share} has a lower value then we say that the solutions are near.
Step 2: Compute the number of solutions N_k and rank of solution R_k as shown in Eq. (47).
Step 3: If $k \propto N$, *k=k+1* then go to step 1. Otherwise, go to step 4 shown in MOGA flow chart 7.
Step 4: Identify max rank R_k.
The assign fitness value is called average fitness value, and given as follows:

$$F_k = N_k - \sum_{k=1}^{R_k+1} \mu(k) - 0.5[\mu(R_k) - 1] \tag{47}$$

Eq. (47) will give average fitness to each solution *k*. Where N_k is total number of solutions, μ_k is number of solutions of the rank R_k, $\mu(R_k)$ are the number of solutions in the current rank. For every solution in the rank, we have to calculate the niche count and as calculated as follows:

Algorithm 2: Pseudo-code of multi-objective genetic algorithm for energy optimization

Inputs:
Population size, max iteration, Boundary conditions, crossover, mutation;
Output:
Optimization of operating cost and pollution emission, and operating cost and availability using RES;
Initialization:
Nk= No of solutions assigned;
Ri= Rank of solutions;
σ_{share}= A constant which determines distance between two solutions;
Step1: Assigning Rank *Rk*=s, where s=1,2,3,.....n;
Step2: Using LMF to assign row fitness to each solution to number of best and worst solutions;
Implementation:
Step3: Choose solutions having rank 1;
Step4: Calculate the average of row fitness value for each rank solutions;
Step5: Assigning fitness to each rank;
step6: Applying mutate;
Fitness assignment to MOGA Choose σ *share*;
Compute *Rk* and *Nk* using equation;
while *iter <Maximum iterations* **do**
  for *Rk=1* **do**
    using equation Rk=1+Nk and check number of solutions having Rk=1;
    Take average of row fitness value of obtained solutions;
    if *k∝N, K=K+1* **then**
      back to step 1 as shown in MOGA flow chart in Fig. 7;
      otherwise, Go to step 4;
    end
    if *Rk= other than 1* **then**
      move to step 1;
      Apply crossover to each assigned values to produce new string;
    end
    if *conditions satisfied* **then**
      Pareto ranks are checked;
      Apply mutate;
    end
  end
  for *Rk=1* **do**
    for *j = 1* **do**
      Getting desired Pareto-fronts ranks;
      Execution go back to step 1 if the following conditions are not satisfied;
    end
  end
end

Table 3
Proposed and existing algorithms convergence assessment.

Algorithms	Iterations	Convergence	Computational time
MOPSO	200	180	40 s
MOGA	200	160	34 s
MOWDO	200	140	29 s

where *k* and *j* are two different solutions which must be in the same rank, *(dkj)* is a share fitness value.

In this work, the computational time of the proposed and existing methods is evaluated in terms of convergence towards the best solution. The results of MOPSO, MOWDO and MOGA algorithms in terms of computational time and convergence rate are listed in Table 3. It is obvious from the results that the number of iterations are set to 200 for the proposed and existing methods, the proposed method converged to the global best solution after 140 iterations while the existing methods (MOGA and MOPSO) converged after 160 and 180 iterations. Thus, the proposed method is faster in terms of convergence to the global best solution because it obtained the global best solution after 140 iterations, which is minimum compared to the existing methods. This faster convergence of the proposed method is due to the optimal section of control parameters like population size, upper and lower bounds, etc.

$$Nc_k = \sum_{j=1}^{\mu(R_k)} sh(dkj) \tag{48}$$

sectionSimulation results, performance evaluations, and discussions

The smart microgrid is connected with a power grid serving three types of consumers residential, industrial and commercial, whose demand load curves are shown in Fig. 8 [52,53]. The proposed optimization model consists of various participants like consumers (residential, commercials and industrials), sources (DGS, PVS, WES, Battery, Grid, MT, FC), and objective functions (operating cost and pollution emission, operating cost and availability) are shown in Fig. 4. The SG is connected with different types of consumers, units, substation and market operation, as shown in Fig. 4. From the weather forecast web site (Willy.Online.Ply.Ltd), the speed of the wind is shown in Fig. 10 [54], which depicts data is collected for two days (48 h). One day has the highest wind speed and the second day has the lowest wind speed.

25 kW SOLAREX MSX solar cells are proposed, containing arrays *(*10×2.5 kW*)* with *h=18.5%* and *s=10* m [55]. Fig. 11 indicates solar

Table 4
Renewable energy sources like wind and solar power generation capacity comparison from the perspective of operating cost and pollution emission with and without involvement in hybrid scheme of DRPS and IBT.

Cases	WES power (kW)	PVS power (kW)	WES power Factor (kW)	PVS power Factor (kW)	Cover percentage of wind power	Cover percentage of solar power
Operating cost without DRPS and IBT	9.11	5.22	57.15	91.47		
Operating cost with DRPS and IBT	7.07	3.03	57.15	91.47	8.2%	31.1%
Pollution emission without DRPS and IBT	51.705	93.32	57.15	91.47		
Pollution emission with DRPS and IBT	45.81	87.05	57.15	91.47	6.8%	2.4%
Simultaneous optimization without DRPS and IBT	25.33	92.11	57.15	91.47		
Simultaneous optimization with DRPS and IBT	20.93	75.13	57.15	91.47	5.1%	13.8%

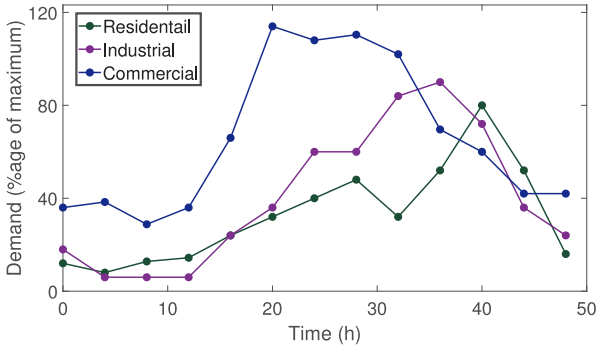

Fig. 8. Daily load curve end-users of residential, commercial, and industrial sectors.

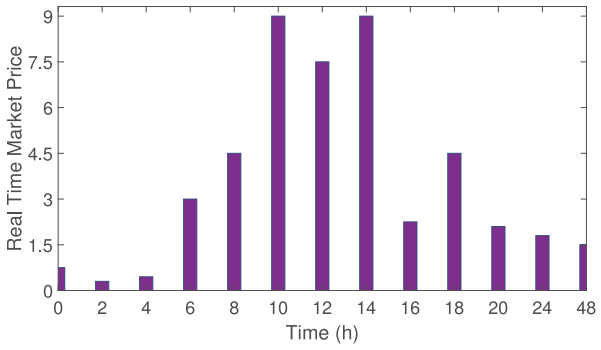

Fig. 9. The real-time market prices of APX.

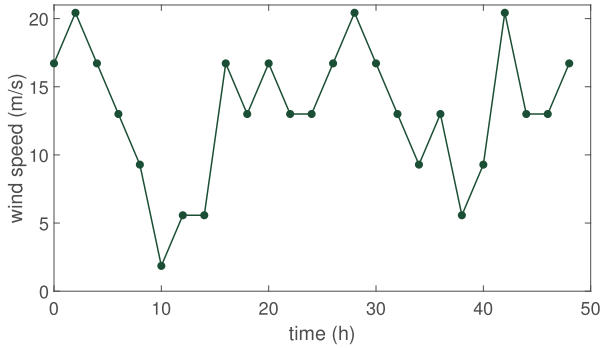

Fig. 10. Wind speed forecasting with hour resolution.

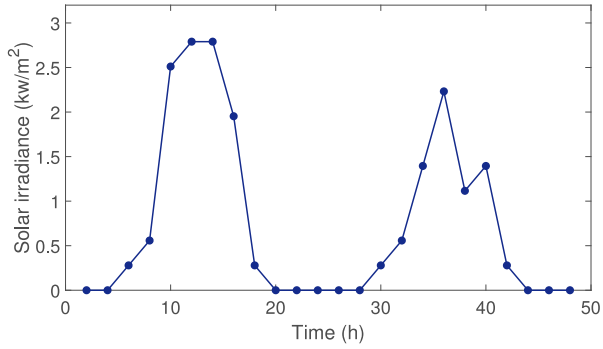

Fig. 11. Solar irradiance forecasting with hour resolution.

irradiance for 48 h period [56]. Solar irradiance is taken for two days: sunny day and cloudy day. The sunny day has high solar irradiance. In contrast, day two, which is cloudy, having a lower intensity of solar irradiance. Both wind and solar energy systems have a power coefficient equal to 1. In contrast, other power sources and loads compensate for the required reactive power through capacitor banks installed on buses. The battery of 30 kWh capacity is considered in this work. The lower and upper limit is adjusted to 15% and 100% of the capacity for discharging and charging, respectively. The state of charge is controlled with efficiency of 95.5% [57,58]. The power consumed is assumed to be 4080 kWh with a 1.33 V/kWh value of load lost. Offered price packages for implementation of the hybrid scheme of DRPS and IBT are listed in Table 1 and the actual market price of APX is shown in Fig. 9. The demand-side consumers, residential, commercial, and industrial, are encouraged to participate in the hybrid scheme of DRPS and IBT.

To evaluate the effectiveness of the proposed model in energy optimization, DRPS+IBT in operating cost, pollution emission, and availability functions, to solve the uncertainty issues caused by solar and wind RES by implementing DRPS and IBT, the evaluation is considered in two different cases as follows.

Case I: Optimization of operating cost and pollution emission with and without involvement in the hybrid scheme of DRPS and IBT.

Case II: Optimization of operating cost and availability with and without involvement in the hybrid scheme of DRPS and IBT.

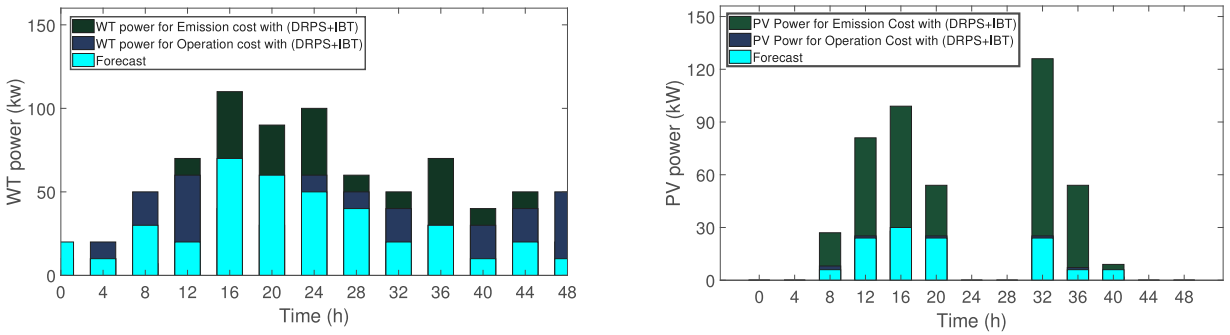

(a) Wind turbine (b) Solar cell

Fig. 12. Output power of renewable energy sources integrated with SG considering operating cost and pollution with involvement in hybrid of scheme of DRPS and IBT).

Table 5
Energy resources optimization without involvement in hybrid DRPS and IBT for operating cost function. Optimized resources like DGS, MT, FC, WES, PVS, battery, and utility are expressed in kW.

Hours	DGS	MT	FC	WES	PVS	Battery	Utility
1	30.000	7.9514	7.283	0.178	0.000	11.587	30.000
2	32.287	12.912	27.010	0.178	0.000	−19.688	26.299
3	45.130	7.189	20.433	0.069	0.000	−19.786	21.963
4	38.075	6.000	24.565	0.000	0.000	−30.000	29.359
5	30.000	8.835	13.956	0.403	0.000	−14.207	26.011
6	37.393	8.068	23.610	0.091	0.000	−21.391	23.818
7	30.000	12.489	19.287	0.016	0.000	−0.705	22.912
8	33.650	9.813	26.953	0.066	0.075	26.505	22.939
9	104.78	28.71	21.210	0.178	0.112	30.000	−30.000
10	234.763	6.000	3.213	0.000	0.000	−15.975	−30.000
11	211.313	8.245	19.145	0.000	0.851	15.444	−30.000
12	283.868	6.000	5.132	0.000	0.000	−30.000	−30.000
13	272.073	6.000	8.400	0.054	1.695	−28.255	−29.966
14	218.992	13.747	24.529	0.473	0.342	21.758	−29.843
15	213.897	14.123	28.932	0.714	0.859	27.265	−29.791
16	226.268	13.190	6.804	0.300	0.338	24.099	−30.000
17	114.225	29.999	29.974	0.000	0.550	30.000	25.252
18	95.459	27.799	30.000	0.741	0.000	30.000	30.000
19	105.819	29.999	30.000	1.302	0.000	30.000	29.879
20	122.196	14.555	29.017	0.000	0.000	26.876	27.355
21	155.728	28.322	28.442	1.300	0.000	30.000	−23.792
22	79.629	28.946	26.685	0.555	0.000	29.860	29.323
23	272.073	6.000	8.400	0.054	1.695	−28.255	−29.966
24	218.992	13.747	24.529	0.473	0.342	21.758	−29.843
25	213.897	14.123	28.932	0.714	0.859	27.265	−29.791
26	226.268	13.190	6.804	0.300	0.338	24.099	−30.000
27	114.225	29.999	29.974	0.000	0.550	30.000	25.252
28	95.459	27.799	30.000	0.741	0.000	30.000	30.000
29	105.819	29.999	30.000	1.302	0.000	30.000	29.879
30	122.196	14.555	29.017	0.000	0.000	26.876	27.355
31	155.728	28.322	28.442	1.300	0.000	30.000	−23.792
32	79.629	28.946	26.685	0.555	0.000	29.860	29.323
33	104.789	28.719	21.210	0.178	0.112	30.000	−30.000
34	234.763	6.000	3.213	0.000	0.000	−15.975	−30.000
35	211.313	8.2457	19.145	0.000	0.851	15.444	−30.000
36	283.868	6.000	5.132	0.000	0.000	−30.000	−30.000
37	272.073	6.000	8.400	0.054	1.695	−28.255	−29.966
38	218.992	13.747	24.529	0.473	0.342	21.758	−29.843
39	213.897	14.123	28.932	0.714	0.859	27.265	−29.791
40	226.268	13.190	6.804	0.300	0.338	24.099	−30.000
41	114.225	29.999	29.974	0.000	0.550	30.000	25.252
42	95.459	27.799	30.000	0.741	0.000	30.000	30.000
43	105.819	29.999	30.000	1.302	0.000	30.000	29.879
44	122.196	14.555	29.017	0.000	0.000	26.876	27.355
45	155.728	28.322	28.442	1.300	0.000	30.000	−23.792
46	79.629	28.946	26.685	0.555	0.000	29.860	29.323
47	54.699	29.097	25.325	0.717	0.000	25.161	30.000
48	31.509	10.515	26.946	0.172	0.000	28.682	25.174

Table 6
Energy resources optimization without hybrid scheme of DRPS and IBT for pollution emission function. The optimized resources like DGS, MT, FC, WES, PVS, battery, and utility are expressed in kW.

Hours	DGS	MT	FC	WES	PVS	Battery	Utility
1	39.654	20.999	32.918	2.428	0.000	31.078	−30.000
2	35.000	26.862	30.000	1.428	0.000	29.518	−28.567
3	35.000	16.837	32.317	2.428	0.000	30.975	−28.547
4	35.105	8.678	28.565	0.781	0.000	30.576	−29.133
5	35.000	9.000	26.000	2.758	0.000	31.988	−32.981
6	35.000	19.279	27.000	0.9146	0.000	31.301	−29.288
7	36.727	29.000	31.678	2.501	0.000	30.735	−28.262
8	55.71	31.000	33.000	2.305	0.275	29.525	−12.000
9	64.526	32.726	29.456	2.630	4.112	30.000	−11.000
10	116.604	30.000	32.000	2.809	12.000	31.975	−20.000
11	129.775	30.000	30.999	11.775	13.851	31.444	−30.000
12	159.640	31.000	30.999	12.410	25.010	31.060	−30.000
13	148.210	28.000	29.988	4.915	21.695	29.245	−29.966
14	223.992	29.000	30.000	3.345	8.342	29.988	−24.843
15	168.908	28.987	30.000	1.980	4.819	32.205	−15.791
16	177.367	31.869	32.019	1.784	0.938	32.080	−19.000
17	165.097	31.999	32.953	1.993	0.550	31.060	−25.252
18	159.091	31.000	33.000	1.985	0.000	31.067	−30.000
19	157.215	27.000	28.812	1.310	0.000	32.340	29.879
20	119.726	29.540	29.986	1.310	0.000	26.886	29.355
21	111.116	29.322	30.000	1.320	0.000	30.800	23.792
22	76.699	31.000	33.000	1.555	0.000	32.810	29.323
23	148.210	28.000	29.988	4.915	21.695	29.245	−29.966
24	223.992	29.000	30.000	3.345	8.342	29.988	−24.843
25	168.908	28.987	30.000	1.980	4.819	32.205	−15.791
26	177.367	31.869	32.019	1.784	0.938	32.080	−19.000
27	165.097	31.999	32.953	1.993	0.550	31.060	−25.252
28	159.091	31.000	33.000	1.985	0.000	31.067	−30.000
29	157.215	27.000	28.812	1.310	0.000	32.340	29.879
30	119.726	29.540	29.986	1.310	0.000	26.886	29.355
31	111.116	29.322	30.000	1.320	0.000	30.800	23.792
32	76.699	31.000	33.000	1.555	0.000	32.810	29.323
33	64.526	32.726	29.456	2.630	4.112	30.000	−11.000
34	116.604	30.000	32.000	2.809	12.000	31.975	−20.000
35	129.775	30.000	30.999	11.775	13.851	31.444	−30.000
36	159.640	31.000	30.999	12.410	25.010	31.060	−30.000
37	148.210	28.000	29.988	4.915	21.695	29.245	−29.966
38	223.992	29.000	30.000	3.345	8.342	29.988	−24.843
39	168.908	28.987	30.000	1.980	4.819	32.205	−15.791
40	177.367	31.869	32.019	1.784	0.938	32.080	−19.000
41	165.097	31.999	32.953	1.993	0.550	31.060	−25.252
42	159.091	31.000	33.000	1.985	0.000	31.067	−30.000
43	157.215	27.000	28.812	1.310	0.000	32.340	29.879
44	119.726	29.540	29.986	1.310	0.000	26.886	29.355
45	111.116	29.322	30.000	1.320	0.000	30.800	23.792
46	76.699	31.000	33.000	1.555	0.000	32.810	29.323
47	48.515	31.573	32.999	0.917	0.000	29.121	31.456
48	41.253	33.227	34.000	0.619	0.000	32.632	−27.674

Table 7
Energy resources optimization with involvement in hybrid scheme of DRPS and IBT for operating cost function. The optimally engaged resources like DGS, MT, FC, WES, PVS, battery, and utility are expressed in kW.

Hours	DGS	MT	FC	WES	PVS	Battery	Utility
1	39.654	10.999	10.918	0.428	0.000	0.768	30.000
2	37.000	11.862	13.00	0.428	0.000	−16.51	26.567
3	36.000	13.837	13.31	0.428	0.000	−19.97	29.547
4	32.105	11.678	21.5	0.781	0.000	−29.57	29.133
5	37.000	8.000	3.000	0.758	0.000	−29.99	3.981
6	39.000	7.279	7.000	0.914	0.000	−21.30	16.288
7	38.727	6.000	25.67	0.50	0.000	−29.73	28.262
8	58.717	10.000	29.000	0.305	0.275	−3.525	2.009
9	67.526	9.726	22.456	0.630	0.112	−20.00	−32.000
10	163.60	20.000	17.000	0.809	0.000	26.975	−32.000
11	229.7	4.000	5.999	0.775	0.851	28.444	−32.000
12	209.64	6.000	15.998	0.410	0.010	18.060	−30.000
13	247.21	5.000	27.988	0.915	0.695	−1.245	−30.966
14	223.99	5.000	5.000	0.345	0.342	−4.988	−34.843
15	268.90	28.987	27.000	0.980	0.819	−7.205	−32.791
16	219.36	15.869	25.019	0.78	0.938	−3.080	−32.000
17	121.09	31.999	29.953	1.99	0.550	11.060	7.252
18	45.091	31.000	29.000	0.98	0.000	5.067	29.000
19	51.215	33.00	30.812	1.31	0.000	30.34	31.879
20	87.726	33.54	28.986	1.31	0.000	27.88	31.355
21	91.116	29.32	24.000	0.32	0.000	25.80	−29.792
22	27.699	18.000	19.000	0.55	0.000	30.81	29.323
23	247.21	5.000	27.988	0.915	0.695	−1.24	−30.966
24	223.99	5.000	5.000	0.345	0.342	−4.98	−34.843
25	268.90	28.987	27.000	0.980	0.819	−7.20	−32.791
26	219.36	15.869	25.019	0.784	0.938	−3.08	−32.000
27	121.09	31.999	29.953	1.993	0.550	11.06	7.252
28	45.091	31.000	29.000	0.985	0.000	5.067	29.000
29	51.215	33.00	30.812	1.310	0.000	30.34	31.879
30	87.726	33.54	28.986	1.310	0.000	27.886	31.355
31	91.116	29.32	24.000	0.320	0.000	25.800	−29.792
32	27.699	18.000	19.000	0.535	0.000	30.810	29.323
33	67.526	9.726	22.456	0.630	0.112	−20.00	−32.000
34	163.60	20.000	17.000	0.809	0.000	26.975	−32.000
35	229.7	4.000	5.999	0.775	0.851	28.444	−32.000
36	209.64	6.000	15.999	0.410	0.010	18.060	−30.000
37	247.21	5.000	27.988	0.915	0.695	−1.245	−30.966
38	223.99	5.000	5.000	0.345	0.3428	−4.988	−34.843
39	268.90	28.987	27.000	0.980	0.8178	−7.205	−32.791
40	219.36	15.869	25.019	0.784	0.938	−3.080	−32.000
41	121.09	31.999	29.953	1.993	0.550	11.060	7.252
42	45.091	31.000	29.000	0.985	0.000	5.067	29.000
43	51.215	33.00	30.812	1.310	0.000	30.340	31.879
44	87.726	33.54	28.986	1.310	0.000	27.886	31.355
45	91.116	29.32	24.000	0.320	0.000	25.800	−29.792
46	27.699	18.000	19.000	0.555	0.00	30.810	29.323
47	4.515	15.573	27.999	0.917	0.000	23.121	31.456
48	29.253	16.22	30.000	0.619	0.000	−22.632	29.674

Table 8
Energy resources optimization with involvement in hybrid scheme of DRPS+IBT for pollution emission function. Optimally engaged resources like DGS, MT, FC, WES, PVS, battery, and utility are expressed in kW.

Hours	DGS	MT	FC	WES	PVS	Battery	Utility
1	29.654	5.999	9.918	0.028	0.000	26.078	−30.000
2	29.000	6.862	23.000	0.328	0.000	28.518	−24.567
3	29.000	11.837	22.317	0.000	0.000	29.975	−27.547
4	29.105	5.678	22.565	0.000	0.000	19.576	−29.133
5	29.000	4.000	23.000	2.758	0.000	30.988	−31.981
6	29.000	6.279	27.000	0.918	0.000	5.301	−29.288
7	31.727	9.000	25.678	0.501	0.000	21.735	−28.262
8	29.717	9.000	33.000	0.305	0.000	29.525	29.000
9	34.526	27.726	29.456	0.630	3.112	29.000	−28.000
10	38.604	26.000	32.000	2.809	7.000	23.975	−20.000
11	76.775	30.000	30.999	10.775	9.851	26.444	20.000
12	100.640	28.000	30.999	16.410	11.010	21.060	15.000
13	148.210	28.000	29.988	2.915	21.695	29.245	29.966
14	42.992	25.000	25.000	1.345	23.342	27.988	1.843
15	129.908	28.987	27.000	2.980	7.819	23.205	15.791
16	126.367	31.869	23.019	1.784	5.938	29.080	19.000
17	165.097	26.999	21.953	1.993	0.550	28.060	30.252
18	77.091	29.000	19.000	1.985	0.000	30.067	5.000
19	57.215	25.000	26.812	1.310	0.000	30.340	23.879
20	59.726	26.540	25.986	1.310	0.000	26.886	18.755
21	67.116	28.322	27.000	1.320	0.000	27.800	29.792
22	41.699	28.000	25.000	1.555	0.000	26.810	17.323
23	148.210	28.000	29.988	2.915	21.695	29.245	29.966
24	42.992	25.000	25.000	1.345	23.342	27.988	1.843
25	129.908	28.987	27.000	2.980	7.819	23.205	15.791
26	126.367	31.869	23.019	1.784	5.938	29.080	19.000
27	165.097	26.999	21.953	1.993	0.550	28.060	30.252
28	77.091	29.000	19.000	1.985	0.000	30.067	5.000
29	57.215	25.000	26.812	1.310	0.000	30.340	23.879
30	59.726	26.540	25.986	1.310	0.000	26.886	18.755
31	67.116	28.322	27.000	1.320	0.000	27.800	29.792
32	41.699	28.000	25.000	1.555	0.000	26.810	17.323
33	75.726	26.540	25.986	1.310	0.000	26.886	18.755
34	70.116	28.322	27.000	1.320	0.000	27.800	29.792
35	71.699	28.000	25.000	1.555	0.000	26.810	17.323
36	83.515	26.573	26.999	0.917	0.000	29.121	18.456
37	61.253	28.227	27.000	0.619	0.000	28.632	−10.674
38	79.654	5.999	9.918	0.028	0.000	26.078	−30.000
39	78.992	25.000	25.000	1.345	23.342	27.988	1.843
40	77.367	31.869	23.019	1.784	5.938	29.080	19.000
41	75.097	26.999	21.953	1.993	0.550	28.060	30.252
42	77.091	29.000	19.000	1.985	0.000	30.067	5.000
43	57.215	25.000	26.812	1.310	0.000	30.340	23.879
44	59.726	26.540	25.986	1.310	0.000	26.886	18.755
45	67.116	28.322	27.000	1.320	0.000	27.800	29.792
46	41.699	28.000	25.000	1.555	0.000	26.810	17.323
47	33.515	26.573	26.999	0.917	0.000	29.121	18.456
48	31.253	28.227	27.000	0.619	0.000	28.632	−10.674

In the cases mentioned above, all the power sources actively participate in the smart microgrid under their ecumenical and technical constraints to coordinate energy exchange with utility and consumers through a PCC to ensure economical, sustainable, secure and reliable operation. The proposed energy optimization model is developed in MATLAB 2017b to solve multi-objective energy optimization problems by catering operational cost and pollution emission, operating cost and availability, simultaneously, with and without involvement in the hybrid scheme of DRPS and IBT.

Case I: Optimization of operating cost and pollution emission with and without involvement in the hybrid scheme of DRPS and IBT.

In this case, first operating cost and pollution emission are optimized without involvement in the hybrid scheme of DRPS and IBT. The optimal engagement of power sources in the smart microgrid to minimize operating cost and pollution emission are listed in Tables 5 and 6, respectively. It is obvious from Table 5 that in early hours where the price of energy is low, the battery must be charged on a priority basis. In contrast, during 9 to 16 h where energy prices are high, the utility purchases energy from the smart microgrid DGs on a priority basis. In this manner, the operational cost is maintained optimized in the proposed model. Similarly, Table 6 results represent that in most cases, the utility purchases energy from DGs of the smart microgrid to ensure minimum pollution emission. Since wind and solar most of the time reach their maximum generation without causing any pollution are considered in pollution emission function, which is shown in Fig. 18(b). On the other hand, these resources offered prices are higher compared to the power sources. Therefore, they are ignored in the optimization of operation cost.

In the second part of case I, the optimization of operational cost and pollution emission with the hybrid scheme of DRPS and IBT is discussed. The power sources are optimally engaged to minimize operation cost and pollution emission, and results obtained are list in Tables 7 and 8, respectively.

From the results presented for case I, it is concluded that the power sources are more optimized with involvement in hybrid scheme DRPS and IBT compared to without involvement case. Comparison results presented in Tables 5 and 7 illustrate that involvement in hybrid scheme DRPS and IBT, production of wind energy reduced from 9.71

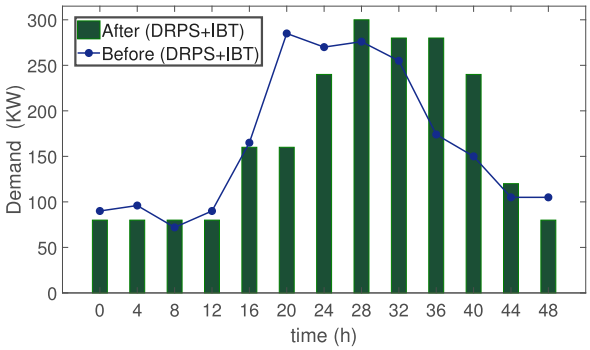

Fig. 13. Consumers load demand with and without implementation of hybrid scheme of DRPS and IBT.

kW to 6.45 kW, and solar power generation reduced from 6.09 kW to 3.20 kW. In contrast, the optimization of emission function with and without involvement in the hybrid scheme of DRPS and IBT shows that the use of hybrid scheme reduces the production of wind from 52.11 kW to 44.48 kW, and from 93.32 kW to 87.13 kW. To visualize the energy produced by solar and WES considering operation cost and emissions with and without involvement in the hybrid scheme are depicted in Figs. 12(a) and 12(b), respectively. Fig. 13 indicates that, in the case of emission function, a hybrid scheme lowers the generation capacity of solar and WES and shifts the load from on-peak to off-peak hours while ensuring the formation of rebound peaks. In this case, the consumers participate in the hybrid scheme of DRPS and IBT and agree that utility will alleviate their energy consumption during specific scheduled hours. It may also allow the utility operator to minimize the scheduled power of power sources and avoid rebound peaks. This behavior of consumers load demand before and after involvement in DRPS and IBT are shown in Fig. 13.

Case II: In case II, the operating cost reduction and availability maximization with and without involvement in the hybrid scheme of DRPS and IBT. The operational cost reduction and availability of RES maximization are evaluated on MOWDO and MOGA algorithms compared to the MOPSO algorithm. The results obtained are graphically presented in Fig. 19, it is obvious that the operating cost is reduced by 7% with involvement in the hybrid scheme of DRPS and IBT and 4% without involvement in the hybrid scheme of DRPS and IBT and the availability of RES is maximized by 15% and 11%, as compared to MOPSO algorithm, respectively. Similarly, the results of Fig. 19 show the convergence characteristics of the MOWDO algorithm to optimize operating cost and maximize the availability of RES. Simulation results show that the operating cost is reduced by 9% and 6% with and without DRPS and IBT, at the same time, the availability of RES is maximized by 20% and 17%, respectively. The convergence characteristics of the MOGA algorithm is shown in Fig. 19. The results of Fig. 19 shows the operating cost reduction and availability maximization with and without involvement in the hybrid scheme of DRPS and IBT. Simulation results show that the operating cost is reduced by 12% and 6% with and without DRPS and IBT, at the same time, the availability of RES is maximized by 25% and 19%, respectively. The comparison of MOPSO, MOWDO and MOGA results are shown in Tables 9 and 10, respectively. From the proposed model, the operating cost reduction and availability of RES maximization are more with involvement in the hybrid scheme of DRPS and IBT compared to existing models and without participation in the hybrid scheme of DRPS and IBT.

From the above-mentioned simulation results of cases I and II, the following discussion is concluded. The proposed energy optimization model optimally allocates power sources in a smart microgrid for simultaneous catering operating cost and pollution emission as two conflicting functions with and without involvement in the hybrid scheme

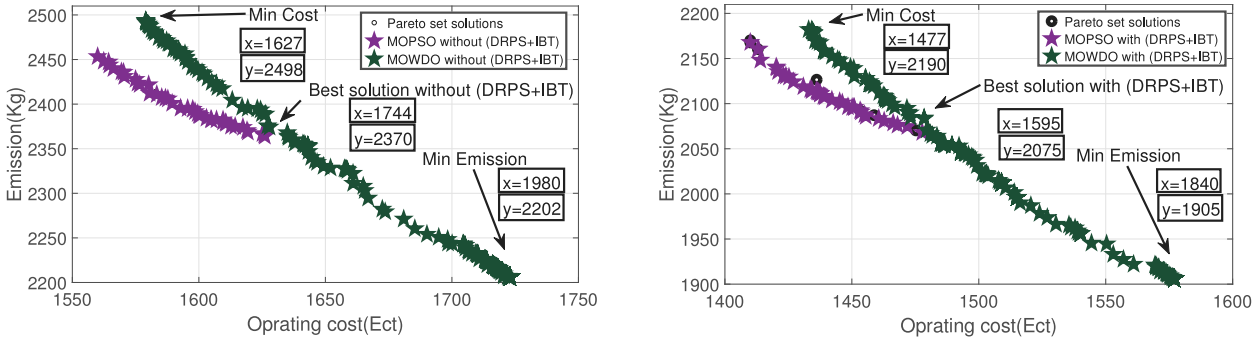

(a) Without hybrid scheme of DRPS and IBT (b) With hybrid scheme of DRPS and IBT)

Fig. 14. Pareto-fronts criterion using MOPSO and MOWDO algorithms for operating cost and pollution emission with/without hybrid scheme of DRPS and IBT.

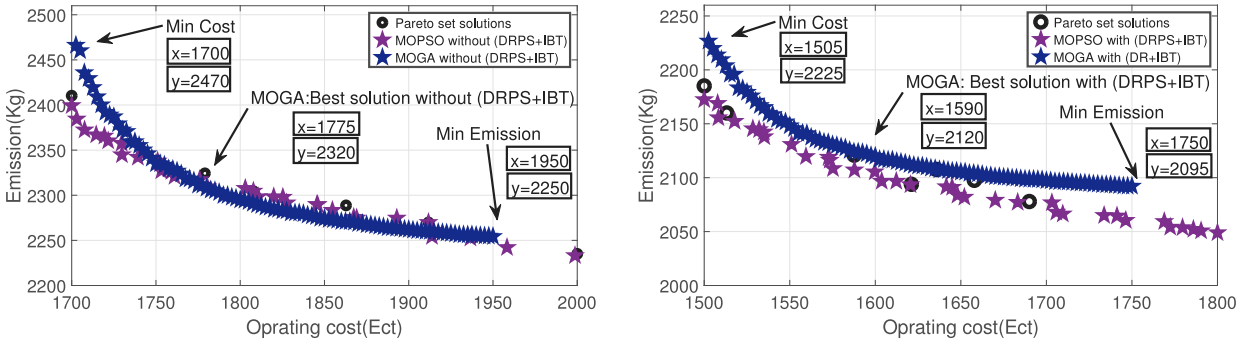

(a) Without hybrid scheme of DRPS and IBT (b) With hybrid scheme of DRPS and IBT

Fig. 15. Pareto-fronts criterion using MOPSO and MOGA algorithms for operating cost and pollution emission with/without hybrid scheme of DRPS and IBT.

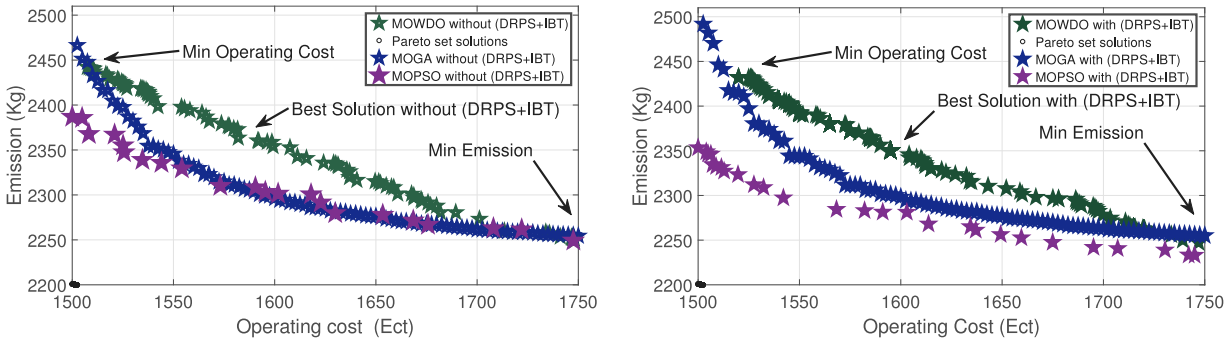

(a) Without hybrid scheme of DRPS and IBT (b) With hybrid scheme of DRPS and IBT

Fig. 16. Pareto-fronts criterion using MOPSO, MOGA, and MOWDO algorithms for operating cost and pollution emission with/without hybrid scheme of DRPS and IBT.

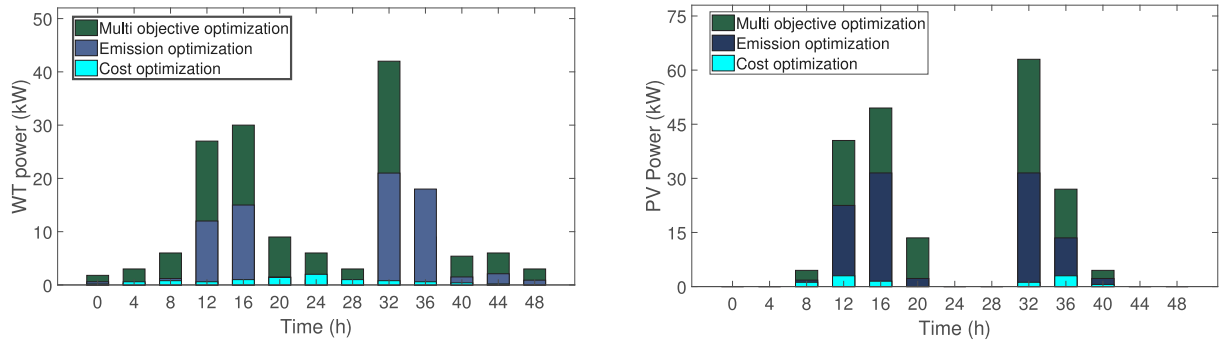

(a) Wind turbine (b) Solar cells

Fig. 17. Renewable energy sources like wind and solar power generation for multi-objective optimization: operating cost and pollution emission.

of DRPS and IBT. According to Figs. 14(a), 14(b), 15(a), 15(b), 16(a) and 16(b), since the operation cost and pollution emission objectives are conflicting, moving from the starting point of the curve towards the endpoint, the Pareto fronts are equal to the change in operating behavior from lowest costs and highest emissions, to highest costs and lowest emissions, where a fuzzy mechanism can compute the optimal operating point and best solutions. Figs. 14(a), 14(b), 15(a), 15(b), 16(a) and 16(b) illustrate that using the hybrid scheme of DRPS and IBT helps to obtain optimal operation point such that where operation cost and pollution emission through MOGA are reduced by 24.5% and 19% and through MOWDO are minimized by 26% and 13% respectively, as compared to MOPSO algorithm.

Figs. 17(a) and 17(b) illustrates that the amount of solar and wind RES minimize operating cost and pollution emission functions, simultaneous minimization of both functions, and ensure avoidance of rebound peaks creation with involvement in the hybrid scheme of DRPS and IBT. Furthermore, it is obvious from the results solar and wind power generation is related to pollution emission function. Therefore, by simultaneous optimization, a balance is established between them. Simulation results listed in Table 4 are for better assessment of output solar and power from the aspects of operating cost and emission with and without involvement in the hybrid scheme of DRPS and IBT. Results depict that in case I, the state of catering operating cost is the optimal state that resolves uncertainty caused by solar and wind power sources. Similarly, for case II, results are listed in 9, which illustrates that the state of considering the availability of RES is the optimal state to resolve uncertainty caused by solar and wind power sources.

Thus, from the above results and discussions, we come across to the conclusion that our developed energy optimization model based on MOWDO and MOGA has outstanding performance compared to the benchmark model in both cases with and without involvement in the hybrid scheme of DRPS and IBT.

4. Conclusion

An energy optimization model based on MOWDO and MOGA is developed for a smart microgrid by considering a novel hybrid scheme of DRPS and IBT as the program to cater to the uncertainty caused by solar and wind power sources of optimization function with conflicting objectives. The operating cost of smart microgrid, availability of RES, and pollution emission caused by different power sources are considered in two separate cases. The probabilistic method is used to model and predict the non-linear and stochastic behavior of solar and wind power generation. To ensure optimal performance of smart microgrid power exchange coordination with the electric utility company and consumers is considered. Furthermore, to control energy consumption and rebound peaks creation, consumers are encouraged to participate in the hybrid scheme of DRPS and IBT via giving incentives in the form of a price offer package. The energy optimization model based on MOWDO and MOGA uses the Pareto criterion and fuzzy mechanism to solve smart microgrid energy optimization problems and obtain an optimal response. Simulation results showed that when consumers participating in the hybrid scheme of DRPS and IBT, the operating cost, pollution emission would likely be minimized, and the availability of RES would be maximized. Results show that in case I, the operating cost and pollution emission with and without DRPS and IBT is minimized by 24.5% and 19% with MOGA, and reduced to 26% and 13% with MOWDO as compared to MOPSO, respectively. Furthermore, in case II, operating cost is reduced by 12% and 6% with and without hybrid DRPS and IBT using MOGA, 13% and 8% using MOWDO compared to MOPSO, respectively. Similarly, the availability of RES is maximized by 20% and 17% using MOGA, 25% and 19% using MOWDO as compared to MOPSO, respectively.

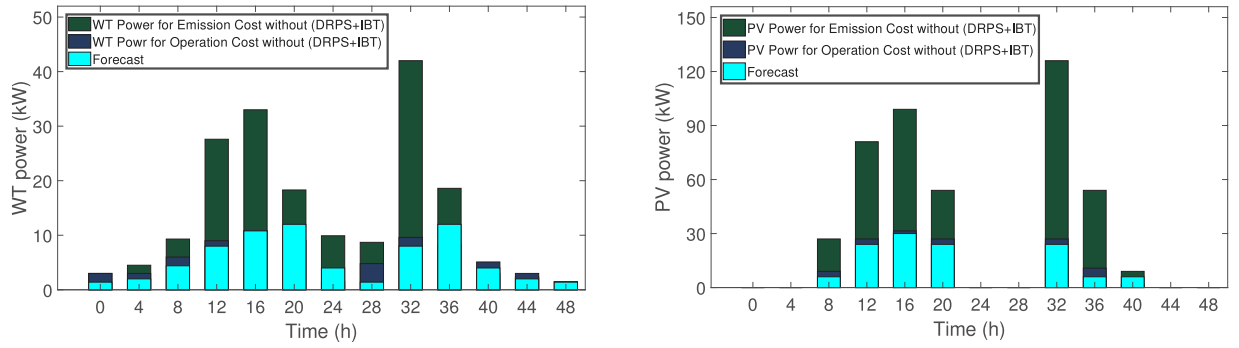

(a) Wind turbine (b) Solar cell

Fig. 18. Output power of renewable energy sources integrated with smart microgrid considering operating cost and pollution without hybrid scheme of DRPS and IBT.

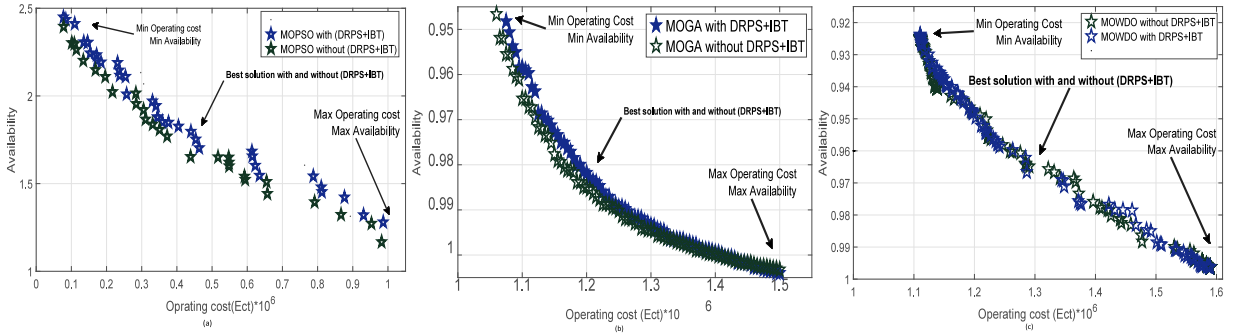

Fig. 19. Pareto-fronts criterion using MOPSO, MOGA, and MOWDO algorithms for operating cost and availability of RES with/without involvement in hybrid scheme of DRPS and IBT.

Table 9
Comparative evaluation of the proposed and existing models in aspects of operating cost and availability without involvement in hybrid scheme of DRPS and IBT.

Techniques	Wind turbine surface area (m^2)	Solar surface area (m^2)	Battery (kW)	Availability index of wind power	Operating cost (Ect)
MOPSO	850	3000	365	98.47%	$1.31*10^6$
MOWDO	700	2870	358	98.17%	$1.33*10^6$
MOGA	690	2660	345	97.44%	$1.2*10^6$

Table 10
Comparative evaluation of the proposed and existing models in aspects of operating cost and availability with involvement in hybrid scheme of DRPS and IBT.

Techniques	Wind turbine surface area (m^2)	Solar surface area (m^2)	Battery (kW)	Availability index of wind power	Operating cost (Ect)
MOPSO	800	2800	340	98.57%	$1.29*10^6$
MOWDO	695	2760	328	98.37%	$1.20*10^6$
MOGA	650	2550	315	97.24%	$1.19*10^6$

This work can be extending in the future by adopting intelligent rule-based techniques and compare them to parametrized cognitive adaptive optimization approach for energy optimization of the smart microgrid.

CRediT authorship contribution statement

Kalim Ullah: Conceptualization, Data curation, Methodology, Writing - original draft, Resources. **Ghulam Hafeez:** Writing - original draft, review & editing, Supervision, Software, Project administration, Visualization, Investigation, Formal analysis, Funding acquisition. **Imran Khan:** Supervision, Project administration, Visualization, Investigation, Writing - review & editing, Formal analysis, Funding acquisition. **Sadaqat Jan:** Writing - review & editing, Formal analysis, Funding acquisition. **Nadeem Javaid:** Supervision, Project administration, Visualization, Investigation, Funding acquisition.

Declaration of competing interest

The authors declare that they have no known competing financial interests or personal relationships that could have appeared to influence the work reported in this paper.

Acknowledgment

The authors extend their sincere appreciation to the University of Engineering and Technology, Mardan, Pakistan, and COMSATS University Islamabad, Islamabad Campus, Pakistan, for funding this research through the Artificial Intelligence in Sustainable Electrical Power, Energy, and Computing (AISEPC) Research group.

References

[1] Ferreira Willian M, Meneghini Ivan R, Brandao Danilo I, Guimarães Frederico G. Preference cone based multi-objective evolutionary algorithm to optimal management of distribuited energy resources in microgrids. Appl Energy 2020;274:115326.

[2] Hakimi Seyed Mehdi, Hajizadeh Amin, Shafie-khah Miadreza, Catalão João PS. Demand response and flexible management to improve microgrids energy efficiency with a high share of renewable resources. Sustainable Energy Technol Assessments 2020;42:100848.

[3] Hasankhani Arezoo, Hakimi Seyed Mehdi. Stochastic energy management of smart microgrid with intermittent renewable energy resources in electricity market. Energy 2020;119668.

[4] Rayati Mohammad, Goghari Sanaz Amirzadeh, Gheidari Zahra Nasiri, Ranjbar AliMohammad. An optimal and decentralized transactive energy system for electrical grids with high penetration of renewable energy sources. Int. J. Electr. Power Energy Syst. 2019;113:850–60.

[5] Hafeez Ghulam, Alimgeer Khurram Saleem, Khan Imran. Electric load forecasting based on deep learning and optimized by heuristic algorithm in smart grid. Appl Energy 2020;269:114915.

[6] Pandit Manjaree, Srivastava Laxmi, Sharma Manisha. Environmental economic dispatch in multi-area power system employing improved differential evolution with fuzzy selection. Appl. Soft Comput. 2015;28:498–510.

[7] Gazafroudi Amin Shokri, Afshar Karim, Bigdeli Nooshin. Assessing the operating reserves and costs with considering customer choice and wind power uncertainty in pool-based power market. Int. J. Electr. Power Energy Syst. 2015;67:202–15.

[8] Vardakas John S, Zorba Nizar, Verikoukis Christos V. Performance evaluation of power demand scheduling scenarios in a smart grid environment. Appl Energy 2015;142:164–78.

[9] Patnam Bala Sai Kiran, Pindoriya Naran M. Demand response in consumer-centric electricity market: mathematical models and optimization problems. Electr. Power Syst. Res. 2020;106923.

[10] Bahmani Ramin, Karimi Hamid, Jadid Shahram. Stochastic electricity market model in networked microgrids considering demand response programs and renewable energy sources. Int. J. Electr. Power Energy Syst. 2020;117:105606.

[11] USDepartment of Energy. Benefits of demand response in electricity markets and recommendations for achieving them. Report to the United States congress. 2006, http://eetd.lbl.gov.

[12] Hafeez Ghulam, Alimgeer Khurram Saleem, Wadud Zahid, Khan Imran, Usman Muhammad, Qazi Abdul Baseer, et al. An innovative optimization strategy for efficient energy management with day-ahead demand response signal and energy consumption forecasting in smart grid using artificial neural network. IEEE Access 2020;8:84415-84433.

[13] Alavi Seyed Arash, Ahmadian Ali, Aliakbar-Golkar Masoud. Optimal probabilistic energy management in a typical micro-grid based-on robust optimization and point estimate method. Energy Convers Manage 2015;95:314–25.

[14] Navid Rezaei, Kalantar Mohsen. Smart microgrid hierarchical frequency control ancillary service provision based on virtual inertia concept: An integrated demand response and droop controlled distributed generation framework. Energy Convers Manage 2015;92:287–301.

[15] Falsafi Hananeh, Zakariazadeh Alireza, Jadid Shahram. The role of demand response in single and multi-objective wind-thermal generation scheduling: A stochastic programming. Energy 2014;64:853–67.

[16] Zakariazadeh Alireza, Jadid Shahram, Siano Pierluigi. Economic-environmental energy and reserve scheduling of smart distribution systems: A multiobjective mathematical programming approach. Energy Convers Manage 2014;78:151–64.

[17] Zakariazadeh Alireza, Jadid Shahram, Siano Pierluigi. Stochastic multi-objective operational planning of smart distribution systems considering demand response programs. Electr. Power Syst. Res. 2014;111:156–68.

[18] Al-Sumaiti Ameena Saad, Ahmed Mohammed Hassan, Rivera Sergio, Moursi Mohammed Shawky El, Salama Mohamed MA, Alsumaiti Tareefa. Stochastic PV model for power system planning applications. IET Renew. Power Gener. 2019;13(16):3168–79.

[19] Mohammadnejad Mehran, Abdollahi Amir, Rashidinejad Masoud. Possibilistic-probabilistic self-scheduling of pevaggregator for participation in spinning reserve market considering uncertain DRPs. Energy 2020;196:117108.

[20] Parvania Masood, Fotuhi-Firuzabad Mahmud. Integrating load reduction into wholesale energy market with application to wind power integration. IEEE Syst J 2011;6(1):35–45.

[21] Aslam Sheraz, Khalid Adia, Javaid Nadeem. Towards efficient energy management in smart grids considering microgrids with day-ahead energy forecasting. Electr. Power Syst. Res. 2020;182:106232.

[22] Cicek Nihan, Delic Hakan. Demand response management for smart grids with wind power. IEEE Trans. Sustain. Energy 2015;6(2):625–34.

[23] Aghajani GR, Shayanfar HA, Shayeghi H. Demand side management in a smart micro-grid in the presence of renewable generation and demand response. Energy 2017;126:622–37.

[24] Aghajani GR, Shayanfar HA, Shayeghi H. Presenting a multi-objective generation scheduling model for pricing demand response rate in micro-grid energy management. Energy Convers Manage 2015;106:308–21.

[25] Aghajani Gholamreza, Ghadimi Noradin. Multi-objective energy management in a micro-grid. Energy Rep. 2018;4:218–25.

[26] Ngoc Phuc Diem Nguyen, Pham Thi Thu Ha, Bacha Seddik, Roye Daniel. Optimal management of wind intermittency in constrained electrical network. Wind Farm: Impact Power Syst Altern Improve Integr 2011;109.

[27] Mohamed Faisal A, Koivo Heikki N. System modelling and online optimal management of microgrid using mesh adaptive direct search. Int. J. Electr. Power Energy Syst. 2010;32(5):398–407.

[28] Mohamed Faisal A, Koivo Heikki N. Multiobjective optimization using mesh adaptive direct search for power dispatch problem of microgrid. Int. J. Electr. Power Energy Syst. 2012;42(1):728–35.

[29] Afshar K, Shokri Gazafroudi A. Application of stochastic programming to determine operating reserves with considering wind and load uncertainties. J Oper Autom Power Eng 2013;23–30.

[30] Mohamed Faisal A, Koivo Heikki N. Online management genetic algorithms of microgrid for residential application. Energy Convers Manage 2012;64:562–8.

[31] Moghaddam Amjad Anvari, Seifi Alireza, Niknam Taher, Pahlavani Mohammad Reza Alizadeh. Multi-objective operation management of a renewable MG (microgrid) with back-up micro-turbine/fuel cell/battery hybrid power source. Energy 2011;36(11):6490–507.

[32] Motevasel Mehdi, Seifi Ali Reza. Expert energy management of a micro-grid considering wind energy uncertainty. Energy Convers Manage 2014;83:58–72.

[33] Alvarez David L, Al-Sumaiti Ameena S, Rivera Sergio R. Estimation of an optimal PV panel cleaning strategy based on both annual radiation profile and module degradation. IEEE Access 2020;8:63832–9.

[34] Sun Yongjun, Ma Rui, Chen Jiayu, Xu Tao. Heuristic optimization for grid-interactive net-zero energy building design through the glowworm swarm algorithm. Energy Build 2020;208:109644.

[35] Rahimi Ehsan, Rabiee Abdorreza, Aghaei Jamshid, Muttaqi Kashem M, Nezhad Ali Esmaeel. On the management of wind power intermittency. Renew. Sustain. Energy Rev. 2013;28:643–53.

[36] Ba Gen. Reliability and Cost/Worth Evaluation of Generating Systems Utilizing Wind and Solar Energy (Ph.D. diss.), University of Saskatchewan; 2005.

[37] Mohamed Faisal A, Koivo Heikki N. System modelling and online optimal management of microgrid using mesh adaptive direct search. Int. J. Electr. Power Energy Syst. 2010;32(5):398–407.

[38] Abouzahr Imad, Ramakumar R. An approach to assess the performance of utility-interactive wind electric conversion systems. IEEE Trans Energy Convers 1991;6(4):627–38.

[39] Atwa YM, El-Saadany EF, Salama MMA, Seethapathy R. Optimal renewable resources mix for distribution system energy loss minimization. IEEE Trans Power Syst 2009;25(1):360–70.

[40] Ettoumi F Youcef, Mefti A, Adane A, Bouroubi MY. Statistical analysis of solar measurements in Algeria using beta distributions. Renew. Energy 2002;26(1):47–67.

[41] Deshmukh MK, Deshmukh SS. Modeling of hybrid renewable energy systems. Renew Sustainable Energy Rev 2008;12(1):235–49.

[42] Tina G, Gagliano S, Raiti S. Hybrid solar/wind power system probabilistic modelling for long-term performance assessment. Solar energy 2006;80(5):578–88.

[43] Shadmand Mohammad B, Balog Robert S. Multi-objective optimization and design of photovoltaic-wind hybrid system for community smart DC microgrid. IEEE Trans Smart Grid 2014;5(5):2635–43.

[44] Mohandes Baraa, Acharya Samrat, Moursi Mohamed Shawky El, Al-Sumaiti Ameena Saad, Doukas Haris, Sgouridis Sgouris. Optimal design of an islanded microgrid with load shifting mechanism between electrical and thermal energy storage systems. IEEE Trans Power Syst 2020;35(4):2642–57.

[45] Chowdhury SP, Chowdhury S, Crossley PA. Islanding protection of active distribution networks with renewable distributed generators: A comprehensive survey. Electr. Power Syst. Res. 2009;79(6):984–92.

[46] Mazzola Simone, Astolfi Marco, Macchi Ennio. A detailed model for the optimal management of a multigood microgrid. Appl Energy 2015;154:862–73.

[47] Kanchev Hristiyan, Lu Di, Colas Frederic, Lazarov Vladimir, Francois Bruno. Energy management and operational planning of a microgrid with a PV-based active generator for smart grid applications. IEEE Trans Ind Electron 2011;58(10):4583–92.

[48] Kennedy James. Encyclopedia of machine learning. Part Swarm Optim 2010;760–6.

[49] Coello CA Coello, Lechuga M Salazar. MOPSO: A proposal for multiple objective particle swarm optimization. In: Proceedings of the 2002 Congress on Evolutionary Computation, Vol. 2. IEEE; 2002, p. 1051–6.
[50] Yang Jie, Ji Zhenping, Liu Shuai, Jia Qiong. Multi-objective optimization based on pareto optimum in secondary cooling and EMS of continuous casting. In: 2016 International Conference on Advanced Robotics and Mechatronics. IEEE; 2016, p. 283–7.
[51] Ishibuchi Hisao, Murata Tadahiko. A multi-objective genetic local search algorithm and its application to flowshop scheduling. IEEE Trans Syst Man Cybern Part C (Appl Rev) 1998;28(3):392–403.
[52] Bouffard François, Galiana Francisco D, Conejo Antonio J. Market-clearing with stochastic security-Part I: formulation. IEEE Trans Power Syst 2005;20(4):1818–26.
[53] Bouffard Francois, Galiana Francisco D, Conejo Antonio J. Market-clearing with stochastic security-Part II: case studies. IEEE Trans Power Syst 2005;20(4):1827–35.
[54] Available online: https://wind.willyweather.com.au/.
[55] The Solar Power Group Company. https://www.enfsolar.com/directory/installer/67081/the-solar-power-group.
[56] Reconstruction and Short-term Forecast of the Solar Irradiance. taken from: https://www.lpc2e.cnrs.fr/en/scientific-activities/plasmas-spatiaux/projects/other-projects-anr-europe-etc/fp7-soteria/.
[57] Chen Changsong, Duan Shanxu, Cai Tong, Liu Bangyin, Hu Gangwei. Smart energy management system for optimal microgrid economic operation. IET Renew Power Gener 2011;5(3):258–67.
[58] Mirzaei Mohammad Javad, Kazemi Ahad, Homaee Omid. RETRACTED: Real-world based approach for optimal management of electric vehicles in an intelligent parking lot considering simultaneous satisfaction of vehicle owners and parking operator. Energy 2014;76:345–56.

KALIM ULLAH has completed his B.Sc. degree in Electrical Engineering from University of Engineering and Technology Peshawar, Pakistan and pursuing M.Sc Electrical Engineering from University of Engineering and Technology, Mardan, Pakistan. Kalim Ullah is working as a Teaching Assistant at the department of Computer Software Engineering, University of Engineering and Technology, Mardan. He has authored or co-authored in 4 peer-reviewed research papers in reputed international journals and conferences. His research interests include: Sustainable and Smart Energy, Cities and Societies, Smart Grids; Applications of Deep Learning and Blockchain in Smart Power Grids; and Stochastic Techniques for Power Usage Optimization in Smart Power Grids etc.

GHULAM HAFEEZ has completed his B.Sc. in Electrical Engineering from University of Engineering and Technology Peshawar, Pakistan and MS and PhD degree in Electrical Engineering from COMSATS University Islamabad, Islamabad, Pakistan. He is lifetime charted engineer from Pakistan Engineering Council. He is working as a Manager University-Industry Linkages/Research Operations & Development in the Directorate of ORIC, University of Engineering and Technology, Mardan. Prior to this, he was Lecturer in Department of Electrical Engineering, University of Engineering and Technology, Mardan. He also worked as a Lecturer University of Wah, Wah Cantt, Pakistan. He has also worked as a Research Associate in COMSATS University Islamabad, Islamabad, Pakistan, where his research focus was Computational Intelligence, Forecast Process, Energy Management, Operation of Electricity Market, and Electric Vehicles in Smart Power Grids. His industrial experience includes working for Alcatel-Lucent and PTCL as Optimization Engineer in Islamabad, Pakistan. He has authored or co-authored in peer-reviewed research papers in reputed international journals and conferences. His research interests include: Sustainable and Smart Energy, Cities and Societies, Smart Grids; Applications of Deep Learning and Blockchain in Smart Power Grids; and Stochastic Techniques for Power Usage Optimization in Smart Power Grids etc.

IMRAN KHAN received the B.Sc. degree in Electrical Engineering from N.W.F.P. University of Engineering and Technology, Peshawar, Pakistan in 2003 and M.Sc. degree in telecommunication engineering from the Asian Institute of Technology, Thailand, in 2007. He did Ph.D. degree at the Telecommunications FOS, School of Engineering and Technology, Asian Institute of Technology, Thailand, in 2010. Currently he is working as professor in Electrical Engineering Department, University of Engineering Technology, Mardan. His research interests include performance analysis of Wireless Communication Systems, OFDM, OFDMA, MIMO, Cooperative Networks, Cognitive Radio Systems, Sustainable and Smart Energy, Cities and Societies, Smart Grids; Applications of Deep Learning and Blockchain in Smart Power Grids; and Stochastic Techniques for Power Usage Optimization in Smart Power Grids etc.

SADAQAT JAN received his Ph.D. degree from Brunel University, London, UK. He is serving as a professor at the Department of Computer Software Engineering, University of Engineering and Technology, Mardan. His research interests include semantic web, data mining, HCI, requirement engineering, and knowledge engineering.

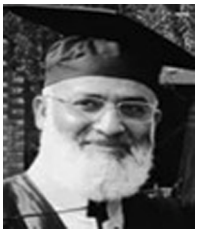

NADEEM JAVAID (Senior Member, IEEE) received the bachelor's degree in computer science from Gomal University, Dera Ismail Khan, Pakistan, in 1995, the master's degree in electronics from Quaid-i-Azam University, Islamabad, Pakistan, in 1999, and the Ph.D. degree from the University of Paris-Est, France, in 2010. He is currently an Associate Professor and the Founding Director of the Communications over Sensors (ComSens) Research Laboratory, Department of Computer Science, COMSATS University Islamabad, Islamabad. He has supervised 126 masters and 20 Ph.D. theses. He has authored over 900 articles in technical journals and international conferences. His research interests include energy optimization in smart/micro grids, wireless sensor networks, big data analytics in smart grids, blockchain in WSNs/smart grids, and so on. He was a recipient of the Best University Teacher Award from the Higher Education Commission of Pakistan, in 2016, and the Research Productivity Award from the Pakistan Council for Science and Technology, in 2017. He is also an Associate Editor of IEEE A ccess and an Editor of the International Journal of Space-Based and Situated Computing and Sustainable Cities and Society.